 

## Editor in Chief - Ulrich Riller

**Editor:** I noted that you are using a lot of abbreviations in the text, in particular for structural geological terms, which normally do not need to be abbreviated, i.e., LANFs and HANFs, and I would advise not to abbreviate these terms. Usually, one should not use more than three abbreviations in a mansucript, as it gets tedious for readers to remember all these while reading a text. For sure you do not need to abbreviate "central Southern Alps", as this term does not appear that often. For the same reason, I would actually refrain from using many, if not all, of the other ones (PDV etc.).

**Reply:** We limited the use of abbreviation, maintaining them for only few cases, to shorten some proper names (e.g. Aga-Vedello LANF).

## Reviewer – Niko Froitzheim

**Reviewer:** The manuscript has been improved substantially. The authors choose not to follow my suggestion that the Pescegallo Fault is the continuation of the Grassi Detachment. I accept this although I do not agree with the argument that the Pescegallo fault and the Grassi detachment should be two different faults because they belong to two different Alpine structural units. If the Alpine thrusts formed in a steeper orientation than the Permian low-angle fault, the latter will occur in more than one Alpine tectonic unit, just like one stratigraphic contact may occur in more than one Alpine structural unit. But as I wrote above, I accept the interpretation.

**Reply:** As we also stressed in the main text, we do not exclude the possibility of a direct connection between the Pescegallo fault and the Grassi detachment We added a brief discussion on this hypothesis. The occurrence of Alpine structures that displaced the Permian ones, hampers the possibility of direct correlation among pre-Alpine structures. The side-by-side occurrence of Permian structures formed at different crustal levels, and currently in contact by Alpine faults, signifies that a direct correlation among Permian structures is at least questionable.

**Reviewer:** Another point of criticism, however, remains: The use of the term "propagation". Propagation means the motion of the tip of a fault leading to the growth of the fault plane. The authors write in the reply that "The framework and the stratigraphic relationships point to a down-section propagation of the Pescegallo fault, which is a typical feature for extensional faults." First, I cannot see how the authors determined the propagation direction, and second, down-section propagation is NOT typical for extensional faults.
The propagation of normal faults was studied in sandbox experiments in this paper:
MARCHAL, D., GUIRAUD, M., RIVES, T. & VAN DEN DRIESSCHE, J. 1998. Space and time propagation processes of normal faults. In: JONES, G., FISHER,Q. J. & KNIPE, R. J. (eds) Faulting, Fault Sealing and Fluid Flow in Hydrocarbon Reservoirs. Geological Society, London, Special Publications, 147, 51-70. The study authors found the following: "Two fundamental types of vertical propagation have been differentiated on the basis of 3D tomographic blocks and kinematic sections (Fig. 9). Upward propagation is most often observed and occurs from the decollement surface (sand/ silicone interface) towards the surface of the model. Downward propagation from the model surface toward the decollement surface is less common." I do not know of any study showing that downward propagation is typical for extensional faults. This point requires correction, also in Fig. 6.

**Reply:** We considered the criticism made by the reviewer and we recognized that the term “propagation” was not the correct one. To avoid misunderstanding, we refrained to use it in the text and in Fig. 6. In our interpretation, we just wanted to stress that, all along its trace, the Pescegallo normal fault preserves young-on-old relationships and constant dip, deepening to the northern quadrants. These features are preserved despite the proximity to the Orobic Thrust and the local re-activation of the fault plane.

### List of Changes to Figures

Fig. 6: we removed the label “down-section propagation”.

# Evidence of Early Permian extension during the post-Variscan evolution of the central Southern Alps (N Italy)

**Sofia Locchi[1,*], Stefano Zanchetta[1], Andrea Zanchi[1]**

1: Dipartimento di Scienze dell'Ambiente e della Terra, Università degli Studi di Milano Bicocca, Piazza della Scienza 4, Milano 20126 - Italy

*Corresponding author's e-mail: s.locchi@campus.unimib.it

## Abstract

In the central Southern Alps (N Italy) some well-preserved Permian extensional structures that exceptionally escaped the Alpine deformation, have been recently identified. Their analysis offers important insights for the interpretation of the post-Variscan tectonics affecting the Southern Alps during the Permian. We describe here a previously unknown fault system related to the development of the Early Permian Orobic Basin, where large exposures of the Variscan basement preserve their original tectonic contacts with the overlying Lower Permian cover. The fault system consists of Low-Angle Normal Faults (LANFs) accompanied by High-Angle Normal faults (HANFs), these last entirely developed within the volcanic, volcaniclastic and terrigenous deposits. The studied structures occurring in the upper part of the Gerola Valley, share several features with Early Permian normal faults already recognized in other areas of the central Southern Alps. The low-angle normal fault planes are characterized by a continuous layer of coarse-grained fault breccias, locally impregnated by tourmalinites. The fault rocks have been invariably observed along the fault surface at the basement-cover contact all across the study area.

This newly identified fault system with its characteristic combination of low- and high-angle normal faults suggests a tectonic regime characterized by pure extension in the central Southern Alps, rather than by a transtensional regime during the Early Permian. The provided data give new insights into

the Early Permian geodynamic scenario, which is discussed in the light of the transition from the Pangea B to the Pangea A configuration.

**Keywords:** Early Permian geodynamics, pure extension, synsedimentary tectonics, Boron metasomatism

# Introduction

The Late Carboniferous to Early Permian post-orogenic evolution of the present-day Alpine region, that followed the Variscan event, was characterized by an intense crustal reorganization (McCann et al. 2006, Stampfli and Kozur 2006; Ziegler et al. 2006). The post-orogenic evolution of the former Variscan hinterland appears to have been strongly controlled by the collapse of the mountain belt, associated to an extensional regime starting in the Early Permian, and resulting in the lithospheric thinning of the Variscan overthickened crust (Brunet and Le Pichon 1982; Brodie and Rutter 1987; Brodie et al. 1989; Prijac et al. 2000; Marotta et al. 2009). Conversely, the former foreland was mostly dominated by late Variscan wrench tectonics in the Stephanian-Autunian times (van Wees et al. 2000), especially along the boundary between the Precambrian and the Phanerozoic Europe (Dadlez et al. 1995).

This transtensional regime active during or just after the orogenic collapse of the Variscan belt is often interpreted to be related to the transition from the Early Permian Pangea B configuration, with Gondwana further to the East (Irving 1977; Muttoni et al. 2013), to the Late Permian Pangea A setting, following a counter-clockwise rotation of Gondwana with respect to Laurasia, as suggested by palaeomagnetic data (Muttoni and Kent 2019). However, this geodynamic interpretation is currently under debate, as progressive evidence point to a different tectonic scenario, dominated by pure extension, at least in the present-day Southern Alps area (e.g. Pohl et al. 2018; Zanchi et al. 2019). From Northern to Southern Europe and in the northernmost portion of Gondwana including the Adria spur (Van Wees et al. 2000; McCann et al. 2006; Timmerman et al. 2009, Zech et al. 2010), the Early

Permian crustal extension was accompanied by HT metamorphism and intense magmatic activity developed at different crustal levels, with emplacement of mafic to intermediate magmatic bodies in the lower crust, intermediate to acid bodies at shallower levels and diffuse volcanic activity at the surface (Fig. 1; Schaltegger and Brack 2007; Schuster and Stüwe 2008). These processes resulted from active rifting, triggered by the progression of lithospheric thinning and asthenospheric upwelling (Diella et al. 1992; Bertotti et al. 1993; Schuster et al. 2001; Stähle et al. 2001; Schuster and Stüwe, 2008; Marotta et al. 2009; Spalla et al. 2014). This general regime of crustal extension led to the development of many intracontinental fault-controlled basins filled by volcanic products, volcaniclastic and terrigenous deposits (Cassinis et al. 2008; Berra et al. 2016). As suggested by the age of volcanism and magmatism, ranging from ca. 290 to 270 Ma (e.g. Schaltegger and Brack 2007), and by the stratigraphic record (Berra and Carminati 2010), the Early Permian subsidence and magmatic activity lasted for a few decades of Ma, representing an episodic event. The Lower Permian units were unconformably sealed by the Upper Permian successions after a sedimentary gap during most of the Middle Permian (Berra and Carminati 2010).

In this paper, we describe a previously unknown Permian fault system related to the opening of these basins that indirectly testifies also for the ongoing magmatic activity. A combination of low- and high-angle normal faults characterizes the structure of the western termination of the Orobic Basin in the upper Gerola Valley, within the northern portion of the central Southern Alps. These newly described normal faults, together with the low-angle normal faults (LANFs) recognized in other locations of the central Southern Alps (Zanchi et al. 2019 and references therein), and the Grassi Detachment Fault in Valsassina (Froitzheim et al. 2008; Pohl et al. 2018) provide a significant contribution for the reconstruction of the Early Permian Orobic Basin architecture. They also support the reconstruction of the extensional setting active during the Early Permian, helping to better understand the tectonic control exerted by the inherited low angle normal faults during the Alpine shortening.

We compare here the Early Permian basins of the central Southern Alps to the orogenic collapse structures of the Basin-and Range Province of the western USA (Lorenz and Nicholls 1984; Menard and Molnar 1988; Schaltegger and Corfu 1995). We suggest that the Orobic Basin, opened by the combination of low- and high-angle normal faults, can be considered as a fossil equivalent of this recent extensional system. For this reason, the analysis of the Permian tectonic structures in the central Southern Alps, preserved as unique relicts of an ancient tectonic history, can also provide important insights on active tectonic extensional contexts.

The tectonic evolution of the Orobic Basin is finally discussed in the frame of the large-scale geodynamic scenario active during the Permian.

# Geological setting

The central Southern Alps (cSA, Fig. 1) are a thick-skinned fold-and-thrust belt grown since the early stages of the Alpine orogeny (Schönborn 1992; Carminati et al. 1997; Zanchetta et al. 2012, 2015). They are characterized by S-vergent structures that nucleated before the onset of the continental collision, between the Late Cretaceous and the Eocene, as suggested by pseudotachylyte $^{49}$Ar/$^{39}$Ar ages obtained along major thrust zones (Zanchetta et al. 2011). The main structures inherited from the Permian and Triassic rifting phases facilitated the development of this fault system (Castellarin et al. 2006) and they deeply involved the pre-Alpine basement, which is now widely exposed in the northern sector as shown in figure 2 (Laubscher 1985; Blom and Passchier 1997; Schönborn 1992; Carminati et al. 1997). The Variscan crystalline basement chiefly consists of two mica-paragneisses and mica-schists ("Morbegno Gneiss" and "Edolo Schists" Auct., respectively, Boriani et al. 2012) with minor lenses of leucocratic orthogneiss ("Gneiss Chiari del Corno Stella" Auct., referred as

Gneiss Chiari through the text and in the figures). Alpine deformations were preceded by the $D_1$ and $D_2$ syn-metamorphic events, which are recorded in the Variscan basement only (Milano et al. 1988; Filippi et al. 2021). The pre-Permian basement was poorly affected by the Alpine metamorphism, reaching in a few localities lower greenschist-facies conditions (Crespi 1981; Spalla et al. 1999; Spalla and Gosso 1999; Carminati and Siletto 2005). The Variscan basement was thrusted to the south on the Permian–Mesozoic sedimentary cover along the Orobic-Porcile-Gallinera thrust (OPGT) system, which extends E-W for more than 80 km (Zanchetta et al. 2015). Moving southward, an array of three basement-cored WSW-ENE–trending anticlines, the "Orobic Anticlines" of De Sitter and De Sitter-Koomans (1949), includes the Lower Permian volcanic, volcaniclastic, and siliciclastic sequence, unconformably covered by the Upper Permian to Lower Triassic units (Forcella and Jadoul 2000; Berra and Siletto 2006). During the Alpine orogenic event, crustal shortening was accommodated by S-SE-vergent thrusting and folding in two distinct stages, $D_3$ and $D_4$, respectively predating and postdating the 42 to 29 Ma intrusion of the Adamello Batholith (Brack 1981; Schönborn 1992; Carminati et al. 1997; Fantoni et al. 2004; D'Adda et al. 2011; Zanchetta et al. 2011, 2015; D'Adda and Zanchetta 2015; Mittempergher et al. 2021). In the northern area of the belt, the basement and the Permian to Lower Triassic successions crop out between the Orobic-Porcile-Gallinera thrust to the north and the Valtorta-Valcanale Fault to the south. This latter separates the Orobic Anticlines from the imbricated thrust sheets consisting of Middle Triassic carbonates (Fig. 2).

The Lower Permian succession of the central Southern Alps was deposited in extensional basins, from west to east, the Orobic, Boario, and Collio basins (Fig. 1). Focusing on the Orobic Basin, the Upper Carboniferous-Permian successions are characterized by the occurrence of two major sedimentary systems. The Lower Permian terrigenous and volcanic units of the Laghi Gemelli Group (Cassinis et al. 1986; Cadel et al. 1996; Boriani et al. 2012; Cassinis et al. 2012; Berra et al. 2016) are unconformably covered by a younger succession, consisting of the Upper Permian continental red beds of the Verrucano Lombardo (Casati and Gnaccolini 1967). The Lower Permian units are, from the bottom, the up to 100 m thick Basal Conglomerate, covered by the up to 800 m thick Cabianca Volcanite (CBV), including large ignimbrite sheets (290 to 270 Ma; Berra et al. 2015). The Cabianca Volcanite is conformably covered by the Pizzo del Diavolo Formation (PDV), which consists of sandstones, siltstones, slates and, along the external portions of the basin, of coarse-grained proximal conglomerates (Mt. Aga Conglomerate to the north, Ponteranica Conglomerate to the west, and Val Sanguigno Conglomerate to the south). These conglomerates interfinger with fine-grained deposits (volcaniclastic sandstone and dark slates) in the depocentral area of the basin. Mixed continental carbonate terrigenous facies occur in the upper part of the Pizzo del Diavolo Formation (Berra et al. 2016). On the base of stratigraphic and tectonic evidence, Berra et al. (2016) suggest that the succession of the Laghi Gemelli Group was deposited in an intracontinental fault-controlled basin developed in semi-arid conditions, strongly recalling the present-day Basin and Range Province. A rich ichnofossil association preserved in the uppermost arenitic-pelitic lithofacies of the Pizzo del Diavolo Formation, interfingering with coarse-grained conglomerates of the same unit ("Conglomerato del Ponteranica" of Casati and Gnaccolini, 1967) in the Gerola Valley, suggests a latest Kungurian age (Petti et al. 2014; Marchetti et al. 2015, Marchetti 2016). Red sandstones and conglomerates of the Verrucano Lombardo (Lopingian?) were deposited above an angular unconformity, testifying to tectonic activity often accompanied by a deep erosion of the Laghi Gemelli Group during the Middle Permian (Casati and Gnaccolini 1967; Berra et al. 2016).

The stratigraphy and architecture of the Orobic Basin reflect the Permian syn-depositional tectonic activity, associated to the development of E-W oriented faults and related facies belts (Casati and Gnaccolini 1967; Cadel et al. 1996). The northern boundary of the basin is defined by the Mt. Aga Conglomerate overlying the Variscan basement along the exceptionally preserved Aga-Vedello LANF. This fault, together with the Masoni LANF, documents the Early Permian extension (Zanchi et al. 2019; Zanchetta et al. 2022), generating asymmetric half-grabens deepening toward the basins depocenters. This low-angle fault system interacted with high-angle normal faults active in the hanging wall during the deposition of the lowermost Pizzo del Diavolo Formation, where co-seismic soft-sediment deformation structures are abundant (Berra and Felletti 2011; Zanchi et al. 2019, 2021; Zanchetta et al. 2022).

The fault planes related to the Permian extensional system are often decorated with cryptocrystalline to aphanitic tourmalinites impregnating cataclasites formed along the basement-cover fault contacts (Zhang et al. 1994; De Capitani et al. 1999; Zanchi et al. 2019; Zanchetta et al. 2022). Tourmalinites were likely formed after circulation of Boron-rich hydrothermal fluids released by the emplacement of granitic and granodioritic bodies in the upper crust (De Capitani et al. 1999) in the 290 – 275 Ma time interval (Pohl et al. 2018). The age of tourmalinite is indirectly constrained, as tourmalinite' clasts occur in the coarse-grained proximal conglomerate of the Pizzo del Diavolo Formation (i.e. Ponteranica Conglomerate, in Zanoni and Spalla 2018). The early erosion of these hydrothermal rocks is consistent with the hypothesis presented by Froitzheim et al. (2008), which suggested that the Ponteranica Conglomerate may represent a syntectonic fan-delta related to the early exhumation of tilted crustal blocks. The severe uplift that occurred during the Middle Permian is testified by the exposure at the surface of Early Permian intrusive bodies in the Valsassina area (Sciunnach 2001; Froitzheim et al. 2008). Here the Upper Permian fluvial conglomerates and sandstones of the Verrucano Lombardo unconformably rest on top of the intrusive bodies and their hosting basement rocks (Casati and Gnaccolini 1967; Sciunnach 2001).

Independent constrains on the age of the Pizzo del Diavolo Formation come from recent biostratigraphic data on ichnofossils association, related to the latest Kungurian, that were found in fine-grained facies of the Pizzo del Diavolo Formation (Marchetti 2016). As abovementioned, these sandstones and slates interfinger with conglomerates, restricting their age to the end of the Kungurian and confirming a late Cisuralian age of this portion of the Pizzo del Diavolo Formation (Marchetti et al. 2015, Marchetti 2016). For this reason, the metasomatic event occurred previously, since tourmalinite' clasts were recognized in the Pizzo del Diavolo Formation conglomerates.

# Methods

This work is based on detailed geological mapping carried out at a 1:5,000 scale, integrated with mesoscopic structural analyses of faults and shear zones exposed in the study area. The results of our fieldwork are synthetized in a new geological map (Fig. 3), where Alpine and Permian structures have been distinguished according to our structural interpretation. Mesoscopic faults and foliations were measured in several sites (Fig. 4a) to reconstruct the relative chronology among different deformational events, as well as fault kinematics. We used kinematic indicators to establish the sense of motion along faults as suggested in Petit et al. (1983), using growth fibres and Riedel secondary fractures when displaced markers were not available. Tension gashes were interpreted according to Hancock (1985). S-C fabrics, foliations and folds were also analysed, and the collected data are shown as stereographic projections (Fig. 4).

Microscopic analyses of the fault rocks sampled along the main tectonic structures complete the fieldwork, with the aim of characterizing the different fabrics developed at the microscale. We devoted particular care to the description and distinction of the possible original fabrics formed during the Permian extension and the ones related to the effects of Alpine deformation, often resulting in a reactivation of older tectonic structures.

# Results

*Alpine deformation*

The most important Alpine structure of this area is the E-W trending Orobic Thrust (sites 1 and 2 of Fig. 4a), along which the Variscan polymetamorphic basement overthrusts the Lower Permian to lowermost Triassic successions (Carminati and Siletto 2005; Zanchetta et al. 2011, 2015). As above mentioned, this thrust is one of the most relevant tectonic structures of the central Southern Alps and it can be clearly recognized eastward, beyond the Forcellino Pass (NE corner of Figs. 3 and 4a). Indeed, the thrust clearly crops out along the trail leading to the pass, forming a duplex between the Variscan Morbegno Gneiss in the hanging wall and the Verrucano Lombardo in the footwall. Two small horses including a thin slice of Gneiss Chiari and conglomerates of the Pizzo del Diavolo Formation (Fig. 5) are juxtaposed between the roof and the floor thrust. Moving from the bottom to the overlying duplex structure, the fault damage zone is progressively characterized by S-C structures indicating a top-to-SE sense of movement along the floor thrust, with foliated cataclasites in the fault core involving both the Gneiss Chiari and the PDV conglomerates. Pseudotachylytes develop especially along the roof thrust within the Morbegno Gneiss (see plots of site 1 and 2, Fig. 4a). Their occurrence was already documented a few kilometres to the east, around the San Marco Pass within the damage zone of the Orobic Thrust (Fig. 2, Zanchetta et al. 2011).

Mesoscopic structures such as S-C shear bands, cataclastic foliations, striated faults and pseudotachylytes show a mean attitude consistent with the thrust orientation, striking ENE-WSW with a NNW dip direction. Mesoscopic faults mainly show dip-slip movements, indicated by kinematic indicators as striations and quartz growth fibres. Alpine deformation in the sedimentary cover is recorded in the Lower Triassic Servino, where the development of close E-W trending disharmonic folds is evident at Pizzo della Nebbia ($PA_3$ and $A_3$ in plot of Fig. 4b).

In the southern part of the study area (Fig. 3), another ENE-WSW striking and N-NW dipping thrust, the Pizzo dei Tre Signori - Avaro Thrust (SAT, named “San Giacomo thrust” in Casati and Gnaccolini, 1967), develops along the northern limb of the Orobic Anticline with a slightly oblique strike compared to the Orobic Thrust (Fig. 3). It extends for more than 20 kilometres from the Biandino Valley (46°00'56.7"N 9°28'16.5"E, out of the map of Fig. 2) to the San Marco Pass (Fig.

2), where it joins the Orobic Thrust interacting with a system of NNE-SSW trending left-lateral transtensional faults, at the centre of figures 3 and 4. The Pizzo dei Tre Signori - Avaro Thrust is another important thrust fault, along which the Variscan basement and the Lower-Permian sedimentary cover overthrust the Verrucano Lombardo and Servino formations in the footwall. Mesoscopic faults occur along this contact at sites 5, 6, and 7 (Fig. 4a), where dip-slip NW-dipping reverse fault surfaces occur both in the hanging wall and in the footwall, and are oriented similarly to the Orobic Thrust. The Pizzo del Diavolo Formation is interested by open folds with ENE-WSW trending hinge, their attitude is consistent with the main structures of the central Southern Alps fold-and-thrust belt (plot of site 10 Fig. 4a). Data on bedding attitude ($S_0$) and Alpine disjunctive cleavage ($S_3$) were collected, and it is noticeable that $S_3$ is developed especially in the most fine-grained portions of the Permian-Triassic sedimentary cover. $S_3$ surfaces along the whole study area strike ENE-WSW and dip to N-NW as $S_0$, but with steeper dip angles ($S_0$ and $S_3$ plotted in figure 4b). During the Alpine shortening, the Permian normal faults were partially inverted; leading to peculiar structural features that will be discussed in the next paragraphs. Subsequent strike-slip, oblique and normal faults crosscut all the previous structures. Two N-S trending oblique normal faults with a left-lateral and a dextral oblique component of motion (plot of site 8, Fig. 4a) are responsible for the additional uplift of the Morbegno Gneiss between the Salmurano Pass and the Lake Pescegallo, forming a horst within the central portion of the study area (Fig. 2, 3 and 4).

*Permian tectonics*

*(i) The Pescegallo Low-Angle Normal Fault*

The Variscan basement cropping out between the Orobic-Porcile-Gallinera Thrust and the Pizzo dei Tre Signori - Avaro Thrust in the upper part of the Gerola Valley (Fig. 4a) tectonically underlies the Pizzo del Diavolo Formation, forming a tectonic window with young-on-old relationships, typically characterizing normal faults. The western boundary of the window is discontinuously exposed from the top of Monte di Sopra down to the Lake Pescegallo and to the Pescegallo village, where it is crosscut by the Orobic-Porcile-Gallinera thrust system (Fig. 3 and Fig. 6). Nice exposures of the fault plane occur close to the southern shore of the Lake Pescegallo, where the Gneiss Chiari and the Pizzo del Diavolo Formation, which respectively represent the lower and upper plates of the extensional system, are in contact along a W-dipping low-angle normal fault, forming a small isolated tectonic window. Fault rocks mainly consist of cataclasites that were later metasomatized with the formation of tourmalinites reaching a thickness of a few decimetres, which strictly follow the fault plane (Fig. 6 and 7). The occurrence of tourmalinites along Early Permian faults zones represents a common feature already described for other fault systems of the same age in the Aga-Vedello area (Zanchi et al., 2019; Zanchetta et al., 2022). Preserved sectors of the fault plane can be followed hundred meters south of the Lake Pescegallo (site 4 in figure 4) towards the northern slopes of Monte di Sopra and around its top (Fig. 3 and 4). Here a thick layer of tourmalinite (Fig. 7c) with a brecciated texture seals the fault surface. Angular clasts (up to few cm large) of the underlying basement chiefly made of polycrystalline quartz and fragments of volcanic rocks, derived from the Lower Permian Cabianca Volcanites, are well recognizable in the outcrop. In this sector, the low-angle normal fault cuts horizontally the summit of Mt. di Sopra (Fig. 3 and 4) isolating a "klippe" forming a sort of "extensional allochthon".

Although some parts of the original low-angle normal fault show a partial inversion due to the Alpine reactivation as reverse faults (Fig. 8), most segments of the exposed fault surface still preserve their original Permian fabrics, characterized by breccias formed at shallow crustal levels, which were later impregnated by Boron-rich fluids. The metasomatic tourmalinization and the subsequent Alpine deformation deeply transformed the texture of the original fault rocks, taking to their present-day cohesive fabrics. Relicts of former coarse-grained breccia textures together with the record of synsedimentary tectonic activity in the hanging wall, suggest that the Pescegallo LANF developed at very shallow depths. Likely at 1-1.5 kilometres, which is the maximum thickness of the Permian succession deposited on top of the fault. The shallow depth of the Pescegallo LANF fits with the general tectonic context, in which the Variscan basement was already exposed at the beginning of the Early Permian, as testified by the composition of the Basal Conglomerate at the base of the succession (Zanoni and Spalla 2018). Evidence of the subsequent Alpine shortening is given by the development of S-C fabric indicating a reverse dip-slip top-to-SE sense of shear, both in the hanging wall and in the footwall of the Pescegallo LANF (Fig. 8a), developed in semi-brittle to brittle conditions. Detailed observations at the outcrop scale (plots of site 4 of Fig. 4) suggest that the identified structures are consistent with the general trend of Alpine ones in this sector of the Southern Alps, which is characterized by S-verging thrusting, as shown by the kinematics of the Orobic-Porcile-Gallinera Thrust (Zanchetta et al. 2011, 2015). However, the low-angle normal fault reactivation was not strong enough to erase the Permian fabrics, as can be observed in Fig. 8b where tourmalinites are still recognizable and can be continuously followed along the fault plane. Similar features occur along the northernmost exposure of the fault planes just above the Pescegallo village, where the low angle normal fault plane is folded in an open asymmetric antiform in response to the Alpine shortening along the Orobic-Porcile-Gallinera Thrust (Fig. 6). In the hanging wall of this segment of the low-angle normal fault, sandstones of the Pizzo del Diavolo Formation lay below the PDV conglomeratic lithofacies (Fig. 6). Despite the likely Alpine reactivation of the fault, young-on-old relationships are still preserved, and the fault planes clearly deepens to the north (Fig. 6).

The Pescegallo LANF is displaced by a N-S trending dip-slip normal fault extending from Monte di Sopra to the Lake Pescegallo to the east and by another N-S trending left-lateral normal fault bounding the Salmurano Pass and the Rocca di Pescegallo (e.g. plot of site 8 of Fig. 4) to the west. Here the contact is exposed to the south of the watershed below the high cliff of Cima Piazzotti, where the low-angle normal fault, still showing preserved younger-on-older relationships (Fig. 9), has been strongly reactivated by the Alpine tectonics and interacts with the Pizzo dei Tre Signori - Avaro Thrust.

### (ii) *The Trona High-Angle Normal Fault (Trona Line)*

In the study area the recognized low-angle normal faults are tectonically related to High-Angle Normal Faults (HANFs), as already observed in adjacent areas (Zanchi et al. 2019), forming a complex syn-depositional faults system that controlled the opening of the Orobic Basin.

The most relevant high-angle normal fault is the Trona Line, originally identified in Casati and Gnaccolini (1967) and in Marchetti et al. (2015). The fault develops with an E-W trend within the Pizzo del Diavolo Formation from the Rocca di Pescegallo up to the Pizzo di Trona (Figs. 3 and 4), running through the Tronella Valley and Lake Rotondo, steeply dipping to the N. The fault marks the boundary between different lithofacies of the Pizzo del Diavolo Formation: well-bedded fine-grained volcanoclastic sandstones to the north and coarse-grained conglomerates (Ponteranica Conglomerate *Auct.*) to the south. Along the fault trace, as will be explained in detail in the next paragraphs, we analysed several mesoscopic small-scale synsedimentary normal faults, suggesting that the Trona Line was active during sedimentation, possibly accompanying the extension along the Pescegallo LANF. A similar low- and high-angle normal fault interaction in the central Southern Alps is reported at Mt. Aga in the nearby upper Brembana Valley, where the development of the Aga Growth Fault (Zanchi et al. 2019) was accompanied by the formation of several mesoscopic synsedimentary normal faults formed in hydroplastic conditions within the fine-grained lithofacies of the Pizzo del Diavolo Formation.

The present-day Trona Line corresponds to a subvertical fault plane resulting from an Alpine reactivation (Fig. 9) and inversion as a high-angle reverse fault in the Tronella Valley (Fig. 4a). Conversely, around Lake Rotondo, the Trona Line shows a southward dipping with normal dip-slip motion (Fig. 12b, plot site 9b).

*Boron metasomatism along the Pescegallo LANF*

In the study area, as in other parts of this sector of the Alps (Zhang et al. 1994, Slack et al. 1996; De Capitani et al. 1999; Zanchi et al. 2019; Zanchetta et al. 2022) the low-angle normal fault planes are invariably decorated with cataclasites frequently transformed into tourmalinites, precipitated from Boron-rich fluids, during or shortly after fault activity.

Tourmalinites are well exposed especially around Lake Pescegallo and in the Monte di Sopra area, invariably marking the main low-angle normal fault plane. Nice outcrops occur just below the summit of Monte di Sopra, where cataclasite and related tourmalinites are up to 40 cm thick (Fig. 7c).

Tourmalinites play a significant role in our reconstruction, since they can be considered as proxies of the coeval Early Permian magmatism and tectonic extensional regime in the central Southern Alps (Zanchetta et al. 2022). Samples coming both from preserved and from reactivated low-angle normal fault' segments have been studied to provide a full characterization of their microstructure and mineralogical composition.

Well-preserved tourmalinites are organized in bands and have generally sharp contacts with the host rock (Fig. 7b). In addition, they are characterized by a different intensity of metasomatic processes both at the macroscopic and microscopic scale (Fig. 10b). Tourmalinites commonly display a dark matrix composed for more than 70% of cryptocrystalline tourmaline, as verified with EDS analyses.

The cataclasites impregnated by the Boron-rich fluids show features and fabrics similar to the ones of the Masoni and Aga-Vedello outcrops (Zhang et al. 1994; Slack et al. 1996; De Capitani et al. 1999; Zanchi et al. 2019, Zanchetta et al. 2022), as they are both matrix and clast-supported, with sub-angular to rounded clasts partially resorbed after fluid-rock interaction (Fig. 10a). The pre-existing clasts form 30% of the tourmaline-impregnated cataclasite and their dimensions range from 10 µm to 3 mm with a mean size of 0.2 mm. They mainly show rounded shapes in the most metasomatized portions of the cataclasites, suggesting that dissolution was active at the expense of fluids circulation, causing mass transfer, a typical effect of metasomatism. In addition, a marked banding with darker and lighter layers is directly related to a higher or lower tourmaline modal content, also testified by the quantity of clasts replaced or preserved by the metasomatic process (Fig. 10b). Tourmalinites include fragments derived from the Variscan basement and the sedimentary cover (Fig. 10c), together with few rounded clasts of former tourmalinites, probably developed during the earlier stages of a long-living circulation of Boron-rich fluids along fault planes. Their occurrence points to polyphasic hydrothermal activity. Among the different clasts, few micrometric subhedral crystals of tourmaline can be found sparse in the matrix, whose identification has been qualitatively checked by EDS-SEM analyses, with a green to brown pleochroism and with high interference colours (Fig. 10e).

Tourmalinites sampled at site 4, which is close to the Orobic Thrust, show a finely foliated fabric in their matrix, with strain caps enriched in opaque minerals around quartz clasts that are associated with strain shadows, filled by quartz, sericite and tourmaline. These microstructural features indicate that a pressure solution mechanism was effective, attesting to dissolution and partial tourmalinites' re-mobilization during the Alpine shortening (Fig. 10d, Philippe et al. 1987; Zanchetta et al. 2022). As above mentioned, a deformation of the tourmalinite is visible at the microscopic scale but it is not strong enough to obliterate the original features of the low-angle normal fault core, which can be still recognized. The obliteration of cataclastic fabrics and the lack of deformation, except for the occurrence of an Alpine reactivation, suggests that tourmalinite formation postdates the main activity of the normal fault, as assumed for the Masoni and the Aga Vedello LANFs (Fig. 2 Zhang et al. 1994; Zanchetta et al. 2022) in the Mt. Masoni and Mt. Aga area.

*Synsedimentary deformation*

Evidence of synsedimentary tectonics, recorded by soft-sediment deformation and small normal faults accompanied by liquefaction structures, has been recognized in the hanging wall of the Pescegallo extensional system. These features occur in several sectors of the study area and are very similar to the synsedimentary structures documented in other parts of the Orobic Basin (Berra and Felletti, 2011; Zanchi et al. 2019; Zanchetta et al. 2022).

Examples of small-scale synsedimentary faults occur in the Pescegallo area within the finest sandy to silty lithofacies of the Pizzo del Diavolo Formation. We analysed decimetric normal faults with a displacement of few centimetres especially close to the Trona Line, where they are concentrated along the shore of Lake Rotondo (site 9 of map in Fig. 4). Similar examples of small-scale conjugate normal fault in association with tension gashes also occur close to Lake Pescegallo (site 3, Fig. 4).

Normal faults show different styles and associations, varying from domino-type systems (e.g. Fig. 11a) to Andersonian conjugate systems accompanied by the development of small horst and grabens at a centimetric scale. All the measured faults show evidence of synsedimentary deformation in hydroplastic conditions testified by dewatering structures at different scales. Plastic folding of laminated layers, flames and small neptunian dikes can be observed in association with these structures. Small faults often crosscut sandy layers, dying out in the fine-grained layers of the unit. At Lake Rotondo (Zanchi et al., 2021), we also observed a small mud volcano with a diapiric structure with a diameter of about 20 centimetres, folding and disrupting the upper sandy beds (e.g. Fig. 11h). Ball-and-pillows, small slumps and disrupted bedding (e.g.: Fig. 11e, f and g) are mostly distributed along the contacts between arenaceous and silty layers.

Rose diagrams including more than 80 fault planes show a dominant ENE-WSW strike with NNW (N330) dip direction and a dip angle ranging mainly from 35° to 75° (Fig. 12a), consistently with the orientation of the Trona Line (see plot site 9). Stress directions suggested by Andersonian conjugate systems and tension gashes are clear evidence of a vertical $\sigma_1$ and a horizontal WNW-ESE trending $\sigma_3$ in present day coordinates.

The occurrence of such structures in the hanging wall of Permian LANFs is consistent with observations carried out in other areas of the northern portion of the central Southern Alps on small-scale synsedimentary faults (Berra et al. 2011; Zanchi et al. 2019; Locchi et al. 2021; Zanchi et al. 2021), which show similar strikes and features including about 500 measured faults.

## Discussion

### *1. The Pescegallo extensional system*

Our analyses performed in the Pescegallo area point to the occurrence of Early Permian extensional faults characterized by a combination of low- and high-angle normal faults systems (Fig. 13a). Several lines of evidence indicate their development. All along the Orobic Thrust, large exposure of the Variscan basement cropping out just below the thrust plane occur only in the Gerola Valley and in the Valsassina area (Froitzheim et al. 2008; Pohl et al. 2018). In both cases, the basement exposure is related to the occurrence of extensional fault systems likely representing the superficial expression of the Early Permian crustal thinning (Filippi at al. 2021 and references therein). In the Gerola Valley area, the tectonic contact between the underlying basement and the sedimentary cover is characterized by young-on-old stratigraphic relationships, suggesting a low-angle normal fault propagating down-section toward the northern quadrants (Fig. 6). This low-angle tectonic contact is defined almost everywhere by coarse-grained cataclasites impregnated with tourmalinites, which have been recognized for the first time in the Pescegallo area all along the fault surface. Metasomatic tourmalinite impregnating cataclasites along low-angle normal faults also occurs in other sectors of the central Southern Alps (Blom and Passchier 1997; Cadel et al. 1996; De Capitani et al. 1999; Zanchi et al. 2019, 2021) like the Aga-Vedello and Masoni LANFs, which have been interpreted as normal faults related to the Early Permian extension (Zanchi et al. 2019). These faults acted as important preferential channels for the circulation of Boron-rich fluids, related to the Early Permian magmatism (Zhang et al. 1994; Slack et al. 1996, De Capitani et al. 1999).

According to the combined mesoscopic and microscopic analyses of the cataclasites developed within the Pescegallo LANF fault core, the presence of remnants of coarse-grained fault breccias with angular to rounded clasts without foliations together with the maximum thickness of the Permian succession (1000-1500 m) suggest a shallow structural environment, not exceeding a few kilometres of depth. Close similarities with the Aga-Vedello LANF, which is also associated to a high-angle synsedimentary fault in its hanging wall ("Aga Growth Fault", Zanchi et al. 2019), and abundant tourmalinite layers along the fault plane (Zhang et al. 1994; Cadel et al., 1996, Blom and Passchier 1997; Zanchi et al. 2019) indicate that the Pescegallo fault, as well, can be related to the Early Permian tectonics. In our interpretation, the Pescegallo LANF is a Permian low-angle normal fault that partially escaped the subsequent Alpine deformation and reactivation. In this framework, the Trona Line is also interpreted as an Early Permian high-angle normal fault (Fig. 13a) active during the deposition of the Pizzo del Diavolo Formation, as suggested by abrupt contacts among different lithofacies and by kinematically coherent mesoscopic synsedimentary normal faults, occurring along the main fault trace.

In addition, the tectonic boundary separating the metamorphic basement from the Lower Permian successions within the deepest portion of the Orobic Anticline (Fig. 2), already noticed by the Dutch geologists ("the Mezzoldo window" in De Sitter and De Sitter Koomans 1949), may represent the lateral equivalent of other components of important extensional systems, directly related to the opening of the Orobic Basin. The Grassi Detachment, identified the Valsassina area to the W of Val Gerola, may represent the deeper expression of this extensional system (Pohl et al. 2018). The Pescegallo fault, in this frame, could represent the upper crustal termination of the Grassi detachment. However, a direct connection of the two fault systems is prevented by the occurrence of Alpine tectonic structures that displaced Early Permian structures and coupled tectonic units that were at different crustal levels during the opening of the Orobic Basin. Compared to the Grassi Detachment, the Gerola extensional system shows different features linked to a shallow crustal environment characterized by brittle deformations, similarly to the Aga-Vedello and Masoni LANFs (Zanchi et al., 2019), which are part of a complex association of low- and high-angle normal faults, active at superficial levels. For these reasons, despite the proximity to the Grassi detachment, we suspect that the Pescegallo LANF belongs to a different structural unit, forming a horse between the Orobic-Porcile-Gallinera Thrust and the Pizzo dei Tre Signori - Avaro Thrust, hampering a direct correlation between the two structures.

The fault attitude, kinematics, fault rocks and the occurrence of tourmalinites suggest all together that the low- and high-angle normal fault system of the Gerola Valley could be considered as part of the original architecture of the fault-controlled extensional Orobic Basin, the opening of which was dominated by low-angle master normal faults with high-angle normal fault nucleating in the hanging wall. In this tectonic frame, the mesoscopic synsedimentary faults affecting the loose water-saturated sandy layers of the Pizzo del Diavolo Formation resulted from tectonic activity, acting in hydroplastic conditions at a maximum depth of few tens of meters from the surface (Obermeier 1996; Montenat et al. 2007) and preceding sediments consolidation and diagenesis along the paleo-Trona Line.

### 2. *The effect of Alpine shortening on Permian structures and structural evolution*

Due to the favourable attitude of most Permian LANFs, which were originally perpendicular to the Alpine direction of shortening, the Alpine deformation partially to completely inverted most of these structures, deleting their original features. However, anomalous stratigraphic relationships, i.e. young-on-old, recognized along some of the major thrust faults of the central Southern Alps, allowed to recognize them as old normal faults reactivated during the Alpine shortening (Blom and Passchier 1997; Zanchetta et al. 2015). The Pescegallo LANF is one of the few examples of preserved Permian normal faults strictly comparable to the Aga-Vedello and Masoni LANFs, which also preserve most of their original Permian features (Zanchi et al. 2019; Zanchetta et al. 2022).

In the studied area, the overprinting effects on the Permian structures by the Alpine tectonics are limited both to the outcrop and to the microscale. Even though the Pescegallo LANF has been folded by the Orobic Thrust in its northern portion (Fig. 4), the reactivation of the fault is generally weak and original fabrics of fault rocks can be still recognized around the area of Lake Pescegallo (Fig. 7c). The effects of the Alpine deformation produced a limited partial inversion accompanied by the formation of S-C fabrics and reverse faults along the main contacts both in the hanging wall and in the footwall around the Lake Pescegallo and Monte di Sopra (site 4, Fig. 8a). Nevertheless, despite the occurrence of the Alpine overprint, tourmalinite layers can be followed all along the reactivated contacts, suggesting a limited amount of the Alpine finite strain, also at the microscopic scale (Fig. 10). During the Alpine event, deformation and inversion were more intensive to the west of the Salmurano Pass and to the south of the watershed below the high cliff of Cima Piazzotti (Fig. 3). Here the former low-angle normal fault only preserves younger-on-older relationships (Fig. 9), whereas the original fault rocks were completely reworked during the Alpine reactivation with the formation of pervasively foliated cataclasites.

The high-angle normal fault, the Trona Line, of the Gerola Valley extensional system was involved as well in the Alpine shortening, but due to its unfavourable attitude it has been only weakly reactivated in terms of displacement, even if with complex motions (Fig. 9).

Based on our geological and structural analyses, we suggest a polyphase evolution of the area (Fig. 13) characterized by a first extensional stage (a) during the Early Permian, leading to the development of low- and high-angle normal faults and controlling the opening and development of the Orobic Basin. These structures were responsible for the final stages of exhumation of the Variscan basement, which was already at shallow crustal level at that time (Filippi et al. 2021 and references therein) in response to the ongoing crustal thinning. Then they have been reactivated and partially inverted during the Alpine shortening (b), that triggered the Orobic Thrust development starting from the Late Cretaceous, at a crustal depth close to the brittle-ductile transition (Zanchetta et al. 2011, 2015).The

Permian normal faults and Alpine thrusts are later crosscut by high-angle normal and strike-slip faults entirely developed in brittle conditions (c), resulting in the final uplift and large exposure of the Variscan basement across the Orobic watershed.

*3. Early Permian pure extension versus transtension in the Southern Alps*

The extensional regime in the Southern Alps, during the Early Permian, was defined based on metamorphic, igneous and structural data obtained from different crustal levels (Marotta et al. 2009; Roda et al. 2019 and references therein). In this geodynamic context, the Early Permian basins are the shallow expression of this extension and they have been generally interpreted to have formed at the end of the Variscan orogenesis in response to a dextral transtension, that affected the whole southern Europe margin and the northern portion of the Gondwanan terranes including Adria (e.g. Arthaud and Matte 1977; Stähle et al. 2001; Cassinis et al. 2008, 2012; Schaltegger and Brack 2007; Muttoni et al. 2009; Gretter et al. 2013). According to paleogeographic reconstructions (Muttoni et al. 2003, 2009; Meijers et al. 2010; Gallo et al. 2017; Muttoni and Kent 2019), this particular tectonic setting is coeval to the activity of a dextral mega-shear zone leading to a Wegenerian Pangea A configuration from a first Pangea B configuration, originally proposed by Irving and Parry (1963) and Irving (1977). In their interpretation, the dextral mega-shear zone active during the Early Permian, was extending across the Southern Europe and the present-day Alpine region, and finally reaching the southern margin of the Palaeotethys to the east. However, this hypothesis is still strongly debated (Pohl et al. 2018; Muttoni and Kent 2019). Field structural evidence supporting the existence of a wrench-tectonics dominated regime related to the opening of the Early Permian basins in the Southern Alps is lacking (Pohl et al. 2018). Most of the authors interpret the Early Permian tectonic setting as the result of a dextral transtension giving origin to pull-apart basins, although no robust evidence of Permian strike-slip faults has been yet documented in the Southern Alps (e.g. Cadel et al. 1996; Schaltegger and Brack 2007 and ref. therein; Berra et al. 2016). Proposed models for the opening and evolution of the Early Permian basins of the Southern Alps are mainly based on the reconnaissance of shallow structures as high-angle conjugate normal faults sets developing horst and graben structures, with E-W faults subparallel to the supposed regional trend of the dextral mega-shear zone (Muttoni et al. 2009).

Field data recently collected in several sectors of the central Southern Alps revealed that the architecture of the Early Permian fault systems was instead characterized by low-angle normal faults, often associated with synthetic high-angle normal faults, possibly accompanied in the western areas by extensional structures developed at deeper crustal levels (e.g. the Grassi Detachment, Froitzheim et al. 2008; Pohl et al. 2018; Zanchi et al. 2019). Both shallow and deep extensional structures along the entire central Southern Alps are consistent with a NW-SE direction of extension in present-day coordinates (Pohl et al. 2018; Zanchi et al. 2019, 2021).

An important aspect of the Early Permian tectonic scenario is the wide distribution of the Permian extensional systems all across southern Europe and northern Gondwana, which points to a large-scale phase of extension and crustal thinning in the latest stage and after the Variscan orogeny (e.g. Rey et al. 1992; Pitra et al 1994; McCann et al. 2006; Roger et al. 2015).

This geodynamic scenario has been since now explained by the above cited dextral mega-shear zone leading from Pangea A to Pangea B configuration (Muttoni et al. 2009 and references therein). As already observed by Pohl et al. (2018) the orientation of the dextral mega-shear displacing the northern margin of Gondwana should be roughly oriented E-W or ENE-WSW resulting at odds with the extensional fault systems identified in the central Southern Alps, which are more consistent with a left-lateral rather than with a right-lateral shear. No evidence of Middle to Late Permian left-lateral shearing have been up to now documented in the Alps and in the Central Europe. This leads to a more complex geodynamic evolution, in which the dextral shearing was likely separated in time from the Early Permian extension. Nevertheless, the Middle Permian sedimentary gap (Jadoul and Gaetani and 1986; Cadel et al., 1996; Cassinis et al. 2012; Sciunnach 2001) followed by the deposition of the Upper Permian Verrucano Lombardo upon the deeply eroded faulted and gently folded Lower

Permian successions (Jadoul and Gaetani 1986; Berra and Felletti, 2011; Berra et al. 2016; Pohl et al. 2018), may be reconciled with the activity of a large scale shear zone causing inversion of the Early Permian basins.

An alternative scenario may involve a strong partitioning between extensional and strike-slip regimes in Southern Europe, producing extensional basin to the south, across the northern portion of Gondwana (e.g. the Orobic Basin in the central Southern Alps) and transtensional basins to the north in the present-day Central Europe area (Montaigne Noire, e.g. Echtler and Malaveille 1990). This scenario has already been proposed by McCann et al. (2006), suggesting a different post-orogenic evolution of the Variscan hinterland (the Alps area and the Southern Alps) and the foreland: a major component of pure extension developed in the hinterland and a wrench tectonics in the foreland, i.e. to the north of the present-days Alps area.

Strong partitioning of deformation in active crustal extensional setting is not uncommon. One of the most studied intracontinental areas undergoing crustal extension is the Basin and Range Province of western North America (e.g. Lister and Davis 1989). Here, the simultaneous activity of low-angle listric normal faults and parallel arrays of steep domino-faults in the hanging wall (Hayman et al. 2003) produces N-S trending grabens and half-grabens dominating the structural setting of the whole region. The tectonic framework of this area is interpreted to derive from a diffuse extensional collapse of the Cordilleran overthickened continental crust of the Western USA in the past 15 My. This scenario is related to the regional stress distribution and orientation induced by the growth of the NW-SE trending right lateral San Andreas Transform Fault (Wernicke et al. 1988; Lister and Davis 1989). The present-day landscape of the Basin and Range Province, with basins filled by Miocene sedimentary and volcanic strata deposited in arid environments (Eaton 1982; Lister and Davis 1989), is likely close to the aspect of the Early Permian intracontinental basins formed in Southern Europe and Northern Gondwana (Menard and Molnar 1988) and in particular within the central Southern Alps (Berra et al. 2016).

The geometry and structural features of the fault-controlled basins in the Basins and Range Province testify to the occurrence of pure extensional half-graben basins in a more complex tectonic frame, with strike-slip dominated tectonics close to the San Andreas Fault (Wernicke et al. 1988, 1989).
The Orobic Basin could be interpreted as an ancient analogue of the modern Basin and Range Province, both from the stratigraphic and structural point of view. In this scenario, pure extensional basins developed before the inception of the activity of the Pangea A to Pangea B dextral mega-shear zone (Muttoni et al. 2009; Muttoni and Kent 2019), as a first post-orogenic response preannouncing the mega-plate reorganization taking to the Wegenerian Pangea A configuration.
It is worth noting that the present-day location of the San Andreas Transform within the Gulf of California strictly follows for more than 1000 kilometres the western margin of the Basin and Range Province, which is represented by the NNW-SSE trending main Gulf escarpment. Dextral faults related to the transform reactivate Late Miocene pure normal faults with dextral motions since Pliocene following a jump of the transform from the continental borderland west of the Baja California Peninsula to the Gulf region (Angelier et al. 1981; Colletta and Angelier 1983; Zanchi 1994; Umhoefer et al. 2020). Following such a geodynamic scenario, a possible parallelism among the inferred Middle Permian dextral mega-shear and the Early Permian extensional structures might be related to their subsequent reactivation in a dextral wrench-dominated regime following previous zones of crustal weakness induced by a generalized extension.

## Conclusions

The Gerola Valley is located in a structural context where Alpine deformation partially overprinted the Early Permian stratigraphic and tectonic features related to the opening of the western part of the Orobic Basin. The main structures of Alpine age in the area are the Orobic Thrust and the Pizzo dei Tre Signori – Avaro Thrust. They developed at shallow crustal level (ca. 12 km depth) and obliterated part of the original Permian tectonic and stratigraphic contacts along their traces. The occurrence of pre-existing favourably oriented low-angle normal faults likely facilitated the propagation of deformation, as testified by their progressively reactivated surfaces. Despite this, several parts of the Early Permian fault system exceptionally escaped the Alpine deformation, allowing to gain insights on the tectonic framework that led to the opening of the intracontinental Orobic Basin.

The main results of this work can be summarized as follows:

- The Gerola Valley shows a well-preserved low- and high-angle normal fault system extending for several kilometres, entirely comparable to other important Permian extensional faults recently identified in the central Southern Alps. This is a typical expression of a stress regime with a vertical $\sigma_1$, suggesting a WNW-ESE direction of extension as dominant mechanism during the Early Permian, at least in the western portion of the Orobic Basin. This interpretation agrees with the orientation of the structures measured along the entire sector, and with the thermal state inferred for the intermediate and deep crust of the Alps in this period, representing the shallow evidence of what happens at deeper crustal levels.
- Similarities with other Permian extensional systems in central Southern Alps are also recognized based on the occurrence of syndepositional active tectonics, testified by growth faults and synsedimentary tectonic structures consistent with the attitude of the Early Permian faults identified in the area.
- Another characteristic feature of the Early Permian faults of the Gerola Valley is the circulation of Boron-rich hydrothermal fluids that precipitated tourmalinites along the low-angle normal fault core impregnating pre-existing fault breccias.
- The temporal and spatial localization of the Permian extensional tectonics strictly recalls the current Basin and Range Province, a modern analogue where a combination of large-scale normal faulting at high and low angles dominates the tectonic scenario.

- Following our results, we suggest that the WNW-ESE oriented extension in present day coordinates all across the central Southern Alps occurred before the transformation from Pangea B to Pangea A, affecting the entire Variscan belt including its forelands. Faults and shear zones formed during this stage may have been reactivated during the transformation of Pangea in a dextral wrench regime, causing basin inversion and the Middle Permian sedimentary gap later sealed by the Upper Permian successions.

**Acknowledgements**

This research was funded by Dipartimento di Scienze dell'Ambiente e della Terra, Università degli Studi di Milano – Bicocca (S. Zanchetta and A. Zanchi). We wish to thank M. I. Spalla and N. Froitzheim for their useful and constructive comments on our draft paper. We are also grateful for the contribution of D. Frigerio and C. Domenighini, respectively master and bachelor students, that collaborated during the fieldwork.

## References

Angelier J., Colletta B., Chorowicz J., Ortlieb L., Rangin C. (1981). Fault tectonics of the Baja California Peninsula and the opening of the Sea of Cortez, Mexico. Journal of Structural Geology, 3(4), 347-357.

Arthaud F., Matte P. (1977). Late Paleozoic strike-slip faulting in southern Europe and northern Africa: Result of a right-lateral shear zone between the Appalachians and the Urals. Geological Society of America Bulletin, 88(9), 1305-1320.

Berra F., Siletto, G. B. (2006). Controllo litologico e stratigrafico sull'assetto strutturale delle Alpi meridionali lombarde: il ruolo degli orizzonti di scollamento. Rendiconti della Società Geologica Italiana, 2, 78-80.

Berra F., Carminati, E. (2010). Subsidence history from a backstripping analysis of the Permo-Mesozoic succession of the Central Southern Alps (Northern Italy). Basin Research, 22(6), 952-975.

Berra F., Felletti F. (2011) "Syndepositional tectonics recorded by soft-sediment deformation and liquefaction structures (continental Lower Permian sediments, Southern Alps, Northern Italy): stratigraphic significance." Sedimentary Geology 235.3-4 (2011): 249-263

Berra F., Tiepolo M., Caironi V., Siletto G. B. (2015). U–Pb zircon geochronology of volcanic deposits from the Permian basin of the Orobic Alps (Southern Alps, Lombardy): chronostratigraphic and geological implications. Geological Magazine, 152(3), 429-443.

Berra F., Felletti, F., Tessarollo, A. (2016). Stratigraphic architecture of a transtensional continental basin in low-latitude semiarid conditions: the Permian succession of the central Orobic Basin (Southern Alps, Italy). Journal of Sedimentary Research, 86(4), 408-429.

Bertotti, G., Siletto, G. B., Spalla, M. I. 1993. Deformation and metamorphism associated with crustal rifting: Permian to Liassic evolution of the Lake Lugano– Lake Como area (Southern Alps). Tectonophysics, 226, 271–284.

Blom J. C., Passchier C. W. (1997). Structures along the Orobic thrust, Central Orobic Alps, Italy. Geologische Rundschau, 86(3), 627-636.

Boriani A., Bini A., Beretta G. P., Bergomi M. A., Berra F., Cariboni M., ... Tognini P. (2012). Note Illustrative della Carta Geologica d'Italia alla scala 1: 50.000. Foglio 056-Sondrio.

Brack P. (1981). Structures in the southwestern border of the Adamello intrusion (Alpi Bresciane, Italy).

Brodie, K. H., Rutter, E. H., 1987. Deep crustal extensional faulting in the Ivrea Zone of Northern Italy. Tectonophysics, 140, 193-212.

Brodie, K.H., Rex, D., Rutter, E.H., 1989. On the age of deep crustal extensional faulting in the Ivrea zone, Northern Italy. Geol Soc London Spec Pub, 45, 203-210.

Brunet M. F., Le Pichon X. (1982). Subsidence of the Paris basin. Journal of Geophysical Research: Solid Earth, 87(B10), 8547-8560.

Cadel G., Cosi M., Pennacchioni G., Spalla M., I., (1996). A new map of the Permo-Carboniferous cover and Variscan metamorphic basement in the Central Orobic Alps, Southern Alps – Italy: structural and stratigraphical data. Mem. Sci. Geol., v. 48, pp 1-53.

Carminati E., Siletto G. B., Battaglia D. (1997). Thrust kinematics and internal deformation in basement- involved fold and thrust belts: The eastern Orobic Alps case (Central Southern Alps, northern Italy). Tectonics, 16(2), 259-271.

Carminati E., Siletto G.B. (2005) - The Central Southern Alps (N. Italy) paleoseismic zone: a comparison between field observations and predictions of fault mechanics. Tectonophysics, 401, 179-197.

Casati P., Gnaccolini M. (1967). Geologia delle Alpi Orobie occidentali. Rivista Italiana di Paleontologia e Stratigrafia, 73, 25-162.

Cassinis G., Dal Piaz G. V., Eusebio A., Gosso G., Martinotti G., Massari F., ... Zerbato M. (1986). Report on a structural and sedimentological analysis in the Uranium province of the Orobic Alps, Italy.

Cassinis G., Cortesogno L., Gaggero L., Perotti C. R., Buzzi L. (2008). Permian to Triassic geodynamic and magmatic evolution of the Brescian Prealps (eastern Lombardy, Italy). Bollettino della Società geologica italiana, 127(3), 501-518.

Cassinis G., Perotti C., Ronchi A. (2012) - Permian continental basins in the Southern Alps (Italy) and peri-mediterranean correlations. International Journal of Earth Sciences, 101, 129-157.

Castellarin A., Vai G. B., Cantelli L. (2006). The Alpine evolution of the Southern Alps around the Giudicarie faults: A Late Cretaceous to Early Eocene transfer zone. Tectonophysics, 414(1-4), 203-223.

Colletta B., Angelier J. (1983). Fault tectonics in northwestern Mexico and opening of the Gulf of California: Bull. Centres Rech. Exlor.-Prod. Elf-Aquitaine, 7(1), 433-446.

Crespi R. (1981). Metamorfismo tardo-alpino di grado bassissimo nel basamento a sud della Linea Insubrica.

D'Adda P., Zanchi A., Bergomi M., Berra F., Malusà M. G., Tunesi A., Zanchetta S. (2011). Polyphase thrusting and dyke emplacement in the central Southern Alps (Northern Italy). International Journal of Earth Sciences, 100(5), 1095-1113.

D'Adda P., Zanchetta S. (2015). Geological-structural map of the Orobic and Porcile thrust junction, central Southern Alps (N Italy). Journal of Maps, 11(1), 25-38.

Dadlez R., Narkiewicz M., Stephenson R. A., Visser M. T. M., Van Wees J. D. (1995). Tectonic evolution of the Mid-Polish Trough: modelling implications and significance for central European geology. Tectonophysics, 252(1-4), 179-195.

De Capitani L., Moroni M., Rodeghiero F. (1999). Geological and geochemical characteristics of Permian tourmalinization at Val Trompia (southern Alps, northern Italy) and relationship with the Orobic tourmalinites. Periodico di Mineralogia, 68, 185-212.

De Sitter L. U., De Sitter-Koomans C. M. (1949). The Geology of the Bergamasc Alps Lombardia Italy. Leidse Geologische Mededelingen, 14(2), 1-257.

Diella, V., Spalla, M. I., Tunesi, A., 1992. Contrasting thermomechanical evolutions in the Southalpine metamorphic basement of the Orobic Alps (Central Alps, Italy). J Metam Geol, 10, 203-219.

Eaton G. P. (1982). The Basin and Range province: Origin and tectonic significance. Annual Review of Earth and Planetary Sciences, 10(1), 409-440.

Echtler H., Malavieille J. (1990). Extensional tectonics, basement uplift and Stephano-Permian collapse basin in a late Variscan metamorphic core complex (Montagne Noire, Southern Massif Central). Tectonophysics, 177(1-3), 125-138.

Fantoni R., Bersezio R., Forcella F. (2004). Alpine structure and deformation chronology at the Southern Alps-Po Plain border in Lombardy. Bollettino della Società geologica italiana, 123(3), 463-476.

Filippi, M., Spalla, M. I., Pigazzini, N., Diella, V., Lardeaux, J. M., Zanoni, D. (2021). Cld-St-And-Bearing Assemblages in the Central Southalpine Basement: Markers of an Evolving Thermal Regime during Variscan Convergence. Minerals, 11(10), 1124.

Forcella F., Jadoul F. (2000). Carta geologica della Provincia di Bergamo alla scala 1: 50.000 con relativa nota illustrativa. Provincia di Bergamo. Bergamo.

Froitzheim N., Derks J.F., Walter J.M., Sciunnach D. (2008). Evolution of an Early Permian extensional detachment fault from synintrusive, mylonitic flow to brittle faulting (Grassi Detachment Fault, Orobic Anticline, southern Alps, Italy). In: Tectonic Aspects of the Alpine-Dinaride-Carpathian System (Siegesmund S., Fugenshuh B. & Froitzheim N., eds). Geological Society, London, Special Publications, 298; 69-82 doi:10.1144/SP298.4.

Gallo L. C., Tomezzoli R. N., Cristallini E. O. (2017). A pure dipole analysis of the Gondwana apparent polar wander path: Paleogeographic implications in the evolution of Pangea. Geochemistry, Geophysics, Geosystems, 18, 1499–1519. https://doi.org/10.1002/2016GC006692

Gretter N., Ronchi A., Langone A., Perotti C. R. (2013). The transition between the two major Permian tectono-stratigraphic cycles in the central Southern Alps: results from facies analysis and U/Pb geochronology. International Journal of Earth Sciences, 102(5), 1181-1202.

Hancock, P. L. (1985) Brittle microtectonics: principles and practices. Journal of Structural Geologv 7,431457.

Hayman N. W., Knott J. R., Cowan D. S., Nemser E., Sarna-Wojcicki A. M. (2003). Quaternary low-angle slip on detachment faults in Death Valley, California. Geology, 31(4), 343-346.

Irving E., Parry L. G. (1963). The magnetism of some Permian rocks from New South Wales. Geophysical Journal International, 7(4), 395-411.

Irving E. (1977) - Drift of the major continental blocks since the Devonian. Nature, 270: 304-309.

Jadoul F., Gaetani M. (1986). L'assetto strutturale del settore lariano centro-meridionale. Memorie della Società Geologica Italiana, 32, 123-131.

Laubscher H. P. (1985). Large-scale, thin-skinned thrusting in the southern Alps: Kinematic models. Geological Society of America Bulletin, 96(6), 710-718.

Lister G.S., Davis G.A. (1989). The origin of metamorphic core complexes and detachment faults formed during Tertiary continental extension in the northern Colorado River region, U.S.A. Journal of Structural Geology, 11, pp. 65-94.

Locchi S., Zanchetta S., Moroni M., and Zanchi A. (2021). Interaction between low-angle normal faults and hydrothermal circulation during Early Permian extensional tectonic in the central Southern Alps, N Italy, EGU General Assembly 2021, online, 19–30 Apr 2021, EGU21-3891, https://doi.org/10.5194/egusphere-egu21-3891.

Lorenz V., Nicholls I. A. (1984). Plate and intraplate processes of Hercynian Europe during the late Paleozoic. Tectonophysics, 107(1-2), 25-56.

Manzotti P., Rubatto D., Zucali M., Korh A. E., Cenki-Tok B., Ballevre M., Engi M. (2018). Permian magmatism and metamorphism in the Dent Blanche nappe: constraints from field observations and geochronology. Swiss journal of geosciences, 111(1), 79-97.

Marchetti L., Ronchi A., Santi G., Voigt S. (2015). The Gerola Valley site (Orobic Basin, Northern Italy): a key for understanding late early Permian tetrapod ichnofaunas. Palaeogeography, Palaeoclimatology, Palaeoecology, 439, 97-116.

Marchetti L. (2016). New occurrences of tetrapod ichnotaxa from the Permian Orobic Basin (Northern Italy) and critical discussion of the age of the ichnoassociation. Papers in Palaeontology, 2(3), 363-386.

Marotta A. M., Spalla M. I., Gosso G. (2009). Upper and lower crustal evolution during lithospheric extension: numerical modelling and natural footprints from the European Alps. Geological Society, London, Special Publications, 321(1), 33-72.

McCann T., Pascal C., Timmermann M. J., Krzywiec P., Lopez-Gomez J., Wetzel A., Krawczyk C. M., Rieke H., Lamarche J. (2006). Post-Variscan (end Carboniferous-Early Permian) basin evolution in Western and Central Europe. In: Gee D. G. & Stephenson R. A. (eds) 2006. European Lithosphere Dynamics. Geological Society, London, Memoirs, 32, 355-388.

Meijers M. J. M., Hamers M. F. van Hinsbergen D. J. J., van der Meer D. G., Kitchka A., Langereis C. G., Stephenson R. A. (2010). New Late Paleozoic paleopoles from the Donbas Foldbelt (Ukraine): Implications for the Pangea A vs. B controversy. Earth and Planetary Science Letters, 297(1-2), 18–33. https://doi.org/10.1016/j.epsl.2010.05.028

Ménard G., Molnar P. (1988). Collapse of a Hercynian Tibetan plateau into a late Palaeozoic European Basin and Range province. Nature, 334(6179), 235-237.

Milano P.F., Pennacchioni G., Spalla M.I. (1988). Alpine and pre- Alpine tectonics in the Central Orobic Alps (Southern Alps). Eclogae Geologicae Helvetiae, 81, 273-293.

Mittempergher S., Zanchi A., Zanchetta S., Fumagalli M., Gukov K., Bistacchi A. (2021). Fault reactivation and propagation in the northern Adamello pluton: The structure and kinematics of a kilometre-scale seismogenic source. Tectonophysics, 806, 228790.

Montenat C., Barrier P., Hibsch C. (2007). Seismites: An attempt at critical analysis and classification. Sedimentary Geology, 196(1-4), 5-30.

Muttoni G., Kent D.V., Garzanti E., Brack P., Abrahamsen N., Gaetani M. (2003). Early Permian Pangaea 'B' to Late Permian Pangaea 'A'. Earth Planet Science Letters, 215, 379-394.

Muttoni G., Mattei M., Balini M., Zanchi A., Gaetani M., Berra F. (2009). The drift history of Iran from the Ordovician to the Triassic. In: South Caspian to Central Iran Basins (Brunet M.-F., Wilmsen M. & Granath J.W., Eds.). Geological Society, London, Special Publications, 312, 7-29.

Muttoni G., Kent D. V. (2019). Adria as promontory of Africa and its conceptual role in the Tethys Twist and Pangea B to Pangea A Transformation in the Permian.

Obermeier, S. F. (1996). Use of liquefaction-induced features for paleoseismic analysis—an overview of how seismic liquefaction features can be distinguished from other features and how their regional distribution and properties of source sediment can be used to infer the location and strength of Holocene paleo-earthquakes. Engineering Geology, 44(1-4), 1-76.

Petit J. P., Proust F., Tapponnier P. (1983). Criteres du sens du mouvement sur les miroirs de failles en roches non calcaires. Bulletin de la Societk geologique de France I, 589-608.

Petti F.M., Bernardi M., Ashley-Ross M.A., Berra F., Tessarollo A., Avanzini, M. (2014). Transition between terrestrial-submerged walking and swimming revealed by Early Permian amphibian trackways and a new proposal for the nomenclature of compound trace fossil. Palaeogeography, Palaeoclimatology, Palaeoecology, 410, 278-289.

Philippe S., Lang-Villemaire C., Lancelot J. R., Girod M., Mercadier H. (1987). Données minéralogiques et isotopiques sur deux gîtes hydrothermaux uranifères du bassin volcano-sédimentaire permien de Collio Orobico (Alpes Bergamasques): mise en évidence d'une phase de remobilisation crétacée. In: Bulletin de Minéralogie, volume 110, 2-3, 1987. Les mécanismes de concentration de l'uranium dans les environnements géologiques.

Pitra P., Burg J. P., Schulmann K., Ledru P. (1994). Late orogenic extension in the Bohemian Massif: petrostructural evidence in the Hlinsko region. Geodinamica Acta, 7(1), 15-30.

Pohl F., Froitzheim N., Obermüller G., Tomaschek F., Schröder O., Nagel T. J., Heuser, A. (2018). Kinematics and age of syn- intrusive detachment faulting in the Southern Alps: Evidence for Early Permian crustal extension and implications for the Pangea A versus B Controversy. Tectonics, 37(10), 3668-3689.

Prijac C., Doin M. P., Gaulier J. M., Guillocheau F. (2000). Subsidence of the Paris Basin and its bearing on the late Variscan lithosphere evolution: a comparison between Plate and Chablis models. Tectonophysics, 323(1-2), 1-38.

Rey P., Burg J. P., Caron J. M. (1992). Middle and Late Carboniferous extension in the Variscan Belt: structural and petrological evidence from the Vosges massif (Eastern France). Geodinamica Acta, 5(1-2), 17-36.

Roda M., Regorda A., Spalla M.I., Marotta A. (2019). What drives Alpine Tethys opening? clues from the review of geological data and model predictions. Geol. J., 54, 2646-2664.

Roger F., Teyssier C., Respaut J. P., Rey P. F., Jolivet M., Whitney D. L., ... Brunel M. (2015). Timing of formation and exhumation of the Montagne Noire double dome, French Massif Central. Tectonophysics, 640, 53-69.

Schaltegger U., Corfu F. (1995). Late Variscan “Basin and Range” magmatism and tectonics in the Central Alps: evidence from U-Pb geochronology. Geodinamica Acta, 8(2), 82-98.

Schaltegger U., Brack P. (2007). Crustal-scale magmatic systems during intracontinental strike-slip tectonics: U, Pb and Hf isotopic constraints from Permian magmatic rocks of the Southern Alps. International Journal of Earth Sciences, 96(6), 1131-1151.

Schönborn G. (1992). Alpine tectonics and kinematic models of the central Southern Alps. Memorie di Scienze Geologiche, 44, 229-393.

Schuster R., Scharbert S., Abart R., Frank W. (2001). Permo-Triassic extension and related HT/LP metamorphism in the Austroalpine–Southalpine realm. Mitt. Ges. Geol. Bergbaustud. Österr, 45, 111-141.

Schuster R., Stüwe K. (2008). Permian metamorphic event in the Alps. Geology, 36(8), 603-606.

Sciunnach D. (2001). Early permian paleofaults at the western boundary of the collio basin (Valsassina, Lombardy). In Permian continental deposits of Europe and other areas. Regional reports and correlations (pp. 37-43). Museo Civico di Science Naturali di Brescia.

Slack J.F., Passchier C.W. & Zhang J.S. (1996). Metasomatic tourmalinite formation along basement-cover décollements, Orobic Alps, Italy. Schweiz. Mineral. Petrogr. Mitt., 76, 193-207.

Spalla M. I., Carminati E., Ceriani S., Oliva A., Battaglia D. (1999). Influence of deformation partitioning and metamorphic re-equilibration on PT path reconstruction in the pre-Alpine basement of central southern Alps (northern Italy).

Spalla M.I., Gosso G. (1999). Pre-Alpine tectonometamorphic units in the central Southern Alps: structural and metamorphic memory. Memorie di Scienze Geologiche, 51, 221-229.

Spalla M. I., Zanoni D., Marotta A. M., Rebay G., Roda M., Zucali M., Gosso G. (2014). The transition from Variscan collision to continental break-up in the Alps: insights from the comparison between natural data and numerical model predictions. Geological Society, London, Special Publications, 405(1), 363-400

Stampfli G. M., Kozur H. W. (2006). Europe from the Variscan to the Alpine cycles. Memoirs-Geological Society of London, 32, 57.

Stähle V., Frenzel G., Hess J. C. 2001. Permian metabasalt and Triassic alkaline dykes in the northern Ivrea zone: clues to the post-Variscan geodynamic evolution of the Southern Alps. Schweizerische Mineralogische und Petrographische Mitteilungen, 81, 1–21.

Timmerman M. J., Heeremans M., Kirstein L. A., Larsen B. T., Spencer-Dunworth E. A., Sundvoll B. (2009). Linking changes in tectonic style with magmatism in northern Europe during the late Carboniferous to latest Permian. Tectonophysics, 473(3-4), 375-390.

Umhoefer P. J., Plattner C., Malservisi R. (2020). Quantifying rates of "rifting while drifting" in the southern Gulf of California: The role of the southern Baja California microplate and its eastern boundary zone. Lithosphere, 12(1), 122-132.

Van Wees J. D., Stephenson R. A., Ziegler P. A., Bayer U., McCann T., Dadlez R., ... Scheck M. (2000). On the origin of the southern Permian Basin, Central Europe. Marine and Petroleum Geology, 17(1), 43-59.

Wernicke B., Axen G. J., Snow J. K. (1988). Basin and Range extensional tectonics at the latitude of Las Vegas, Nevada. Geological Society of America Bulletin, 100(11), 1738-1757.

Wernicke B. P., Snow J. K., Axen G. J., Burchfiel B. C., Hodges K. V., Walker J. D., Guth P. L. (1989). Extensional Tectonics in the Basin and Range Province between the southern Sierra Nevada and the Colorado Plateau. In 28th International Geological Congress Field Trip Guidebook (Vol. 138, p. 80).

Zanchetta S., D'Adda P., Zanchi A., Barberini V., Villa I. M. (2011). Cretaceous-Eocene compressions in the central Southern Alps (N Italy) inferred from 40Ar/39Ar dating of pseudotachylytes along regional thrust faults. Journal of Geodynamics, 51, 245-263, doi: 10.1016/j.jog.2010.09.004.

Zanchetta S., Garzanti E., Doglioni C., Zanchi A. (2012). The Alps in the Cretaceous: a doubly vergent pre- collisional orogen. Terra Nova, 24(5), 351-356.

Zanchetta S., Malusà M., Zanchi A. (2015). Precollisional development and Cenozoic evolution of the Southalpine retrobelt (European Alps). Lithosphere, 7, 662-681.0.

Zanchetta S., Locchi S., Carminati G., Mancuso M., Montemagni C., Zanchi A. (2022). Metasomatism by Boron-Rich Fluids along Permian Low-Angle Normal Faults (Central Southern Alps, N Italy). Minerals, 12(4), 404.

Zanchi A. (1994). The opening of the Gulf of California near Loreto, Baja California, Mexico: from basin and range extension to transtensional tectonics. Journal of Structural Geology, 16(12), 1619-1639.

Zanchi A., Zanchetta S., Berio L., Berra F., Felletti, F. (2019). Low-angle normal faults record Early Permian extensional tectonics in the Orobic Basin (Southern Alps, N Italy). Italian Journal of Geosciences, 138(2), 184-201.

Zanchi A., Locchi S., Zanchetta S. (2021). Early Permian syndepositional tectonics in the Orobic Basin, Southern Alps, Italy, EGU General Assembly 2021, online, 19–30 Apr 2021, EGU21-8056, https://doi.org/10.5194/egusphere-egu21-8056.

Zanoni D., Spalla M. I. (2018). The Variscan evolution in basement cobbles of the Permian Ponteranica Formation by microstructural and petrologic analysis. Italian Journal of Geosciences, 137(2), 254-271.

Zech J., Jeffries T., Faust D., Ullrich B., Linnemann U. (2010). U/Pb-dating and geochemical characterization of the Brocken and the Ramberg Pluton, Harz Mountains, Germany. Geologica Saxonica, 56, 9-24.

Zhang J.S., Passchier C.W., Slack J. F. (1994). Cryptocrystalline Permian tourmalinites of possible metasomatic origin in the Orobic Alps, Northern Italy. Economic Geology, 89, 391-396.

Ziegler, P. A., Schumacher, M. E., Dèzes, P., Van Wees, J. D., & Cloetingh, S. A. P. L. (2006). Post-Variscan evolution of the lithosphere in the area of the European Cenozoic Rift System. Geological Society, London, Memoirs, 32(1), 97-112.

## Figure captions

**Fig. 1 –** Map representing the Permian lower crust, intrusive bodies, volcanics, and sedimentary cover identified in the Southern Alps (N Italy). The names of the intracontinental fault-controlled basins formed during the Early Permian extensional phases are, from W to E, Orobic, Boario, Collio, Tione, Tregiovo, Forni-Avoltri and Pramollo Basins. The Orobic Basin, our study area, is in the central Southern Alps (cSA). AVD = Athesian Volcanic District.

**Fig. 2** - Structural setting of the northern portion of the cSA, the black square indicates the location of Fig. 3. Blue faults are related to the Permian evolution of the Orobic Basin (LANF, Low-Angle Normal Fault, modified after Zanchi et al., 2019) and the red ones to the Alpine event.

**Fig. 3** - Geological map of the Gerola Valley from Casati and Gnaccolini (1967) and from our own data surveyed at a 1:5,000 scale. Cross sections AA' and BB', shown in Fig. 6 and 9, were selected

to illustrate the architecture of the Permian faults. Yellow stars indicate the position of studied samples with tourmalinites.

**Fig. 4 –** a) Geological and structural map with the structural data related to key sites. Sites 1 and 2 are along the Orobic Thrust; in site 4 the reactivation of the Pescegallo LANF can be observed; sites 5, 6 and 7 are close to the Pizzo dei Tre Signori-Avaro Thrust; in site 8, two N-S trending oblique normal faults respectively with a left-lateral and a dextral oblique component of motion are responsible for the horst of the Morbegno Gneiss between the Salmurano Pass and the Lake Pescegallo; in site 10 open folds with ENE-WSW axial planes and hinges develop in the Pizzo del Diavolo Formation. b) plot with bedding attitude $S_0$ and Alpine disjunctive cleavage $S_3$, developed in the Permian-Triassic sedimentary cover, together with close disharmonic E-W trending folds at Pizzo della Nebbia. Sites 3 and 9 are reported in Fig. 12. Fault planes are given projected as cyclographics with fault striations and sense of motion; coloured points are poles to foliations; see legend for additional details. Discussion of the data is in the text.

**Fig. 5** - Panoramic view of the Forcellino Pass, with the Orobic Thrust (OT) trace and duplex structures developed along the main fault plane. The yellow inset shows a detail of the OT fault core cropping out along the trail: it is mainly composed of foliated cataclasites with pseudotachylytes at the contact between Gneiss Chiari and Pizzo del Diavolo Fm (PDV).

**Fig. 6** - Cross-section AA' going from the Lake Pescegallo to the summit of Mt. di Sopra. The low-angle normal fault surface is progressively reactivated getting closer to the Alpine Orobic Thrust, where cataclastic foliation and S-C bands develop across the fault zone (see Fig. 8) preserving the young-on-old relationships. However, the reactivation is not so pervasive, the lithofacies variation of PDV can be appreciated and, according to the stratigraphic relationships, it suggests that the deepening of the basin controlled by the activity of the low-angle normal fault is to the north.

**Fig. 6 –** Tourmalinites exposed in the Gerola Valley, along the low-angle normal fault core. The plots represent the attitude of the Pescegallo LANF at Lake Pescegallo and at Mt. di Sopra. Their different attitude suggests a deformation of the original plane. a) At the Lake Pescegallo, the tectonic window represented in cross section AA' (Fig. 6) provides the exposure of the low-angle normal fault core, with cataclasites permeated by tourmalinites, which are shown in detail in b). c) Below Mt. di Sopra, a metre thick layer of tourmalinite separates the Variscan basement from the Lower Permian sedimentary cover and it is composed of several generations of tourmalinite veins, suggesting a multiphase fluids circulation. d) Fault core detail, characterized by cataclased basement and sedimentary cover. Clasts are cut by different generation of Boron-rich fluids precipitating tourmalinites.

**Fig. 8 –** a) At site 4 the reactivation of the Pescegallo LANF generates an S-C fabric, both in the hangingwall and the footwall, and different C' shear planes. They show a displacement with top-to-the-south and are consistent with the kinematics of the Orobic Thrust (see plots of sites 1 and 4 of Fig. 4). b) Close to site 4, a cleavage occurs and develops especially in the fine-grained cataclasites and in the finest portions of the PDV. The tourmalinite bands are poorly deformed, as obvious at the microscale (Fig. 10d).

**Fig. 9 –** Cross section BB'; the trace is shown in Fig. 3. The trace crosses the Pescegallo LANF and the Trona Line, here showing a strong reactivation with a partial inversion. The Pescegallo LANF maintains the young-on-old relationship and the Trona Line abruptly separates different lithofacies of the PDV. The Pizzo dei Tre Signori-Avaro Thrust (SAT) juxtaposes the Variscan basement onto the Permian cover, involving some tectonic slices of Verrucano Lombardo.

**Fig. 10 –**Tourmalinites observed at the optical (transmitted light) and electronic microscope (f). a) The tourmalinite is composed of a homogeneous fine-grained dark matrix as discernible at plane polarized light, with more than 70% of cryptocrystalline tourmaline and clasts from the cataclasites;

b) layers with different intensity of tourmalinization visible at plane polarized light, with a higher concentration in the darker portions; c) clasts derived from the cataclasis of the Variscan basement and of the Lower Permian sedimentary cover, easily distinguishable at crossed polarized light. The vertical veins are filled with carbonate; d) tourmalinites sampled close to site 4 are deformed after Alpine shortening and the mechanism of pressure solution is active in the matrix, whereas strain shadows develop around the clasts, as discernible at plane polarized light. The distribution of these features suggests an anisotropic deformation; e) tiny tourmaline crystal at crossed polarized light; f) BSE image of small tourmaline crystals sparse in the matrix.

**Fig. 11 –** Examples of synsedimentary structures close to Lake Rotondo (site 3 of Fig. 4a). a), b), c), d) Synsedimentary mesoscopic normal faults organized in domino systems; e), f), g) disrupted strata; h) extrusive structure along a small mud volcano.

**Fig. 12 –** a) Rose diagram related to the synsedimentary mesoscopic normal faults measured at sites 3 and 9 around Lake Rotondo. b) Overview of site 9, with the trace of the normal fault (site 9b) nucleated close to the Trona Line and the position of the measured synsedimentary faults (site 9a and 9c); c) Plots of the data related to mesoscopic synsedimentary normal faults, collected at sites 3 and 9.

**Fig. 13** -Evolutionary steps interpreted from the field data analysed in the present study. a) Early Permian stage during which an extensional regime led to the development of low- and high-angle normal fault system, responsible for the opening of the intracontinental Orobic Basin. b) Alpine stage $D_3$ with compressional regime that partially reactivated and inverted the Permian structures developing just a cataclastic foliation and -C fabric. c) Late-Alpine stage, during which all the previous structures have been crosscut by N-S normal to oblique faults, resulting in an additional uplift of the Variscan basement forming an horst.

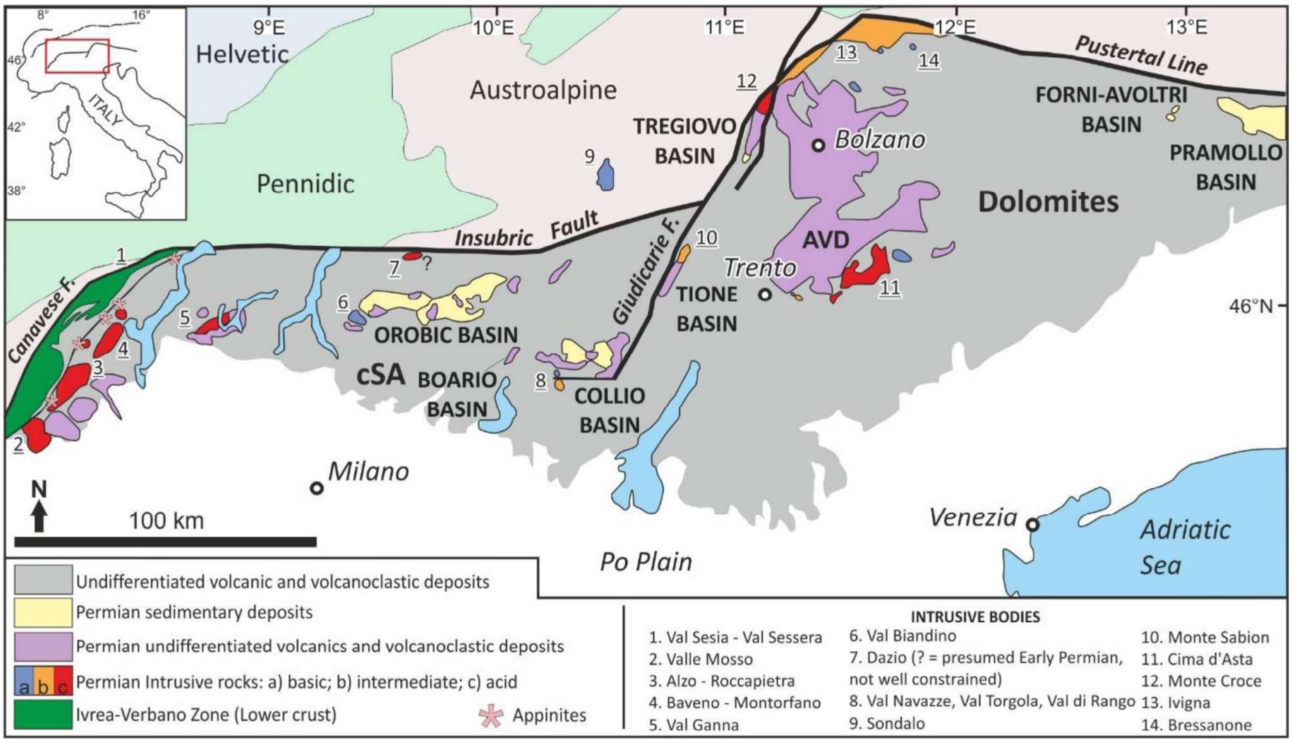

Helvetic
Austroalpine
Pennidic
TREGIOVO BASIN
FORNI-AVOLTRI BASIN
PRAMOLLO BASIN
Pustertal Line
Bolzano
Dolomites
AVD
Insubric Fault
Giudicarie F.
Trento
TIONE BASIN
Canavese F.
OROBIC BASIN
cSA
BOARIO BASIN
COLLIO BASIN
Milano
100 km
Venezia
Po Plain
Adriatic Sea
46°N
9°E
10°E
11°E
12°E
13°E
Undifferentiated volcanic and volcanoclastic deposits
Permian sedimentary deposits
Permian undifferentiated volcanics and volcanoclastic deposits
Permian Intrusive rocks: a) basic; b) intermediate; c) acid
Ivrea-Verbano Zone (Lower crust)
Appinites
INTRUSIVE BODIES
1. Val Sesia - Val Sessera
2. Valle Mosso
3. Alzo - Roccapietra
4. Baveno - Montorfano
5. Val Ganna
6. Val Biandino
7. Dazio (? = presumed Early Permian, not well constrained)
8. Val Navazze, Val Torgola, Val di Rango
9. Sondalo
10. Monte Sabion
11. Cima d'Asta
12. Monte Croce
13. Ivigna
14. Bressanone


**Fig. 1**

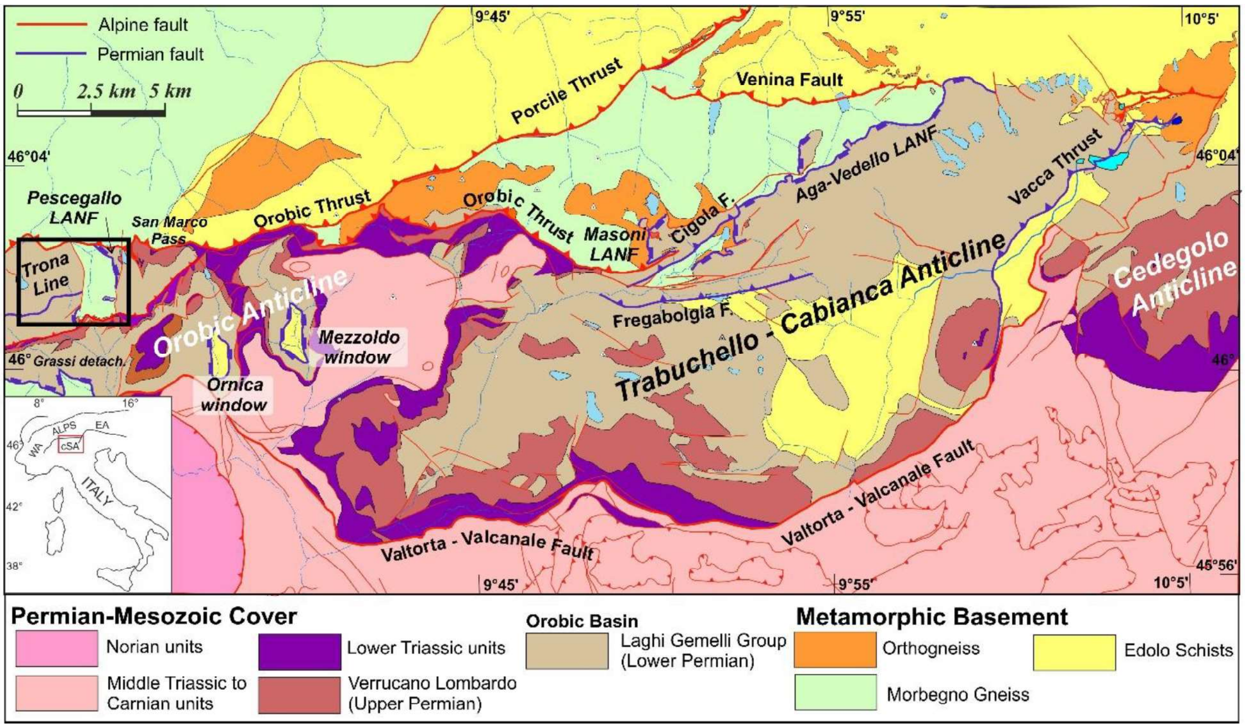

Alpine fault
Permian fault
0 2.5 km 5 km
Porcile Thrust
Venina Fault
Aga-Vedello LANF
Vacca Thrust
Pescegallo LANF
San Marco Pass
Orobic Thrust
Masoni LANF
Cigola F.
Trona Line
Orobic Anticline
Mezzoldo window
Ornica window
Grassi detach.
Fregabolgia F.
Trabuchello - Cabianca Anticline
Cedegolo Anticline
Valtorta - Valcanale Fault
9°45'
9°55'
10°5'
46°04'
46°
45°56'
Permian-Mesozoic Cover
Norian units
Middle Triassic to Carnian units
Lower Triassic units
Verrucano Lombardo (Upper Permian)
Orobic Basin
Laghi Gemelli Group (Lower Permian)
Metamorphic Basement
Orthogneiss
Morbegno Gneiss
Edolo Schists


**Fig.2**

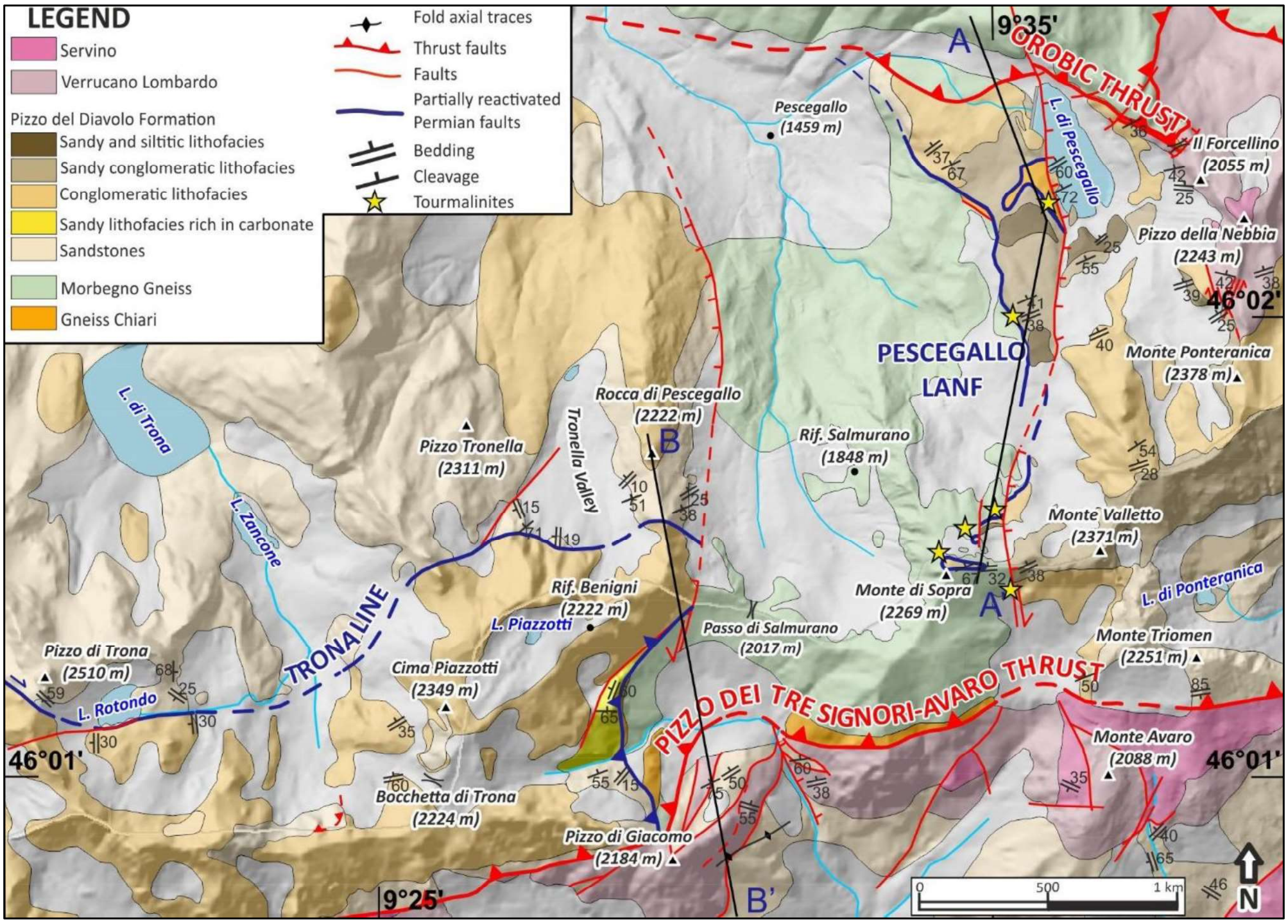

LEGEND
Servino
Verrucano Lombardo
Pizzo del Diavolo Formation
Sandy and siltitic lithofacies
Sandy conglomeratic lithofacies
Conglomeratic lithofacies
Sandy lithofacies rich in carbonate
Sandstones
Morbegno Gneiss
Gneiss Chiari
Fold axial traces
Thrust faults
Faults
Partially reactivated Permian faults
Bedding
Cleavage
Tourmalinites
OROBIC THRUST
PESCEGALLO LANF
TRONA LINE
PIZZO DEI TRE SIGNORI-AVARO THRUST
Pescegallo (1459 m)
Il Forcellino (2055 m)
Pizzo della Nebbia (2243 m)
Monte Ponteranica (2378 m)
Rocca di Pescegallo (2222 m)
Pizzo Tronella (2311 m)
Tronella Valley
Rif. Salmurano (1848 m)
Monte Valletto (2371 m)
Monte di Sopra (2269 m)
Rif. Benigni (2222 m)
Passo di Salmurano (2017 m)
Monte Triomen (2251 m)
Pizzo di Trona (2510 m)
Cima Piazzotti (2349 m)
Bocchetta di Trona (2224 m)
Pizzo di Giacomo (2184 m)
Monte Avaro (2088 m)
L. di Trona
L. Zancone
L. Rotondo
L. Piazzotti
L. di Pescegallo
L. di Ponteranica
9°35'
9°25'
46°02'
46°01'
A
A'
B
B'
0
500
1 km
N


**Fig. 3**

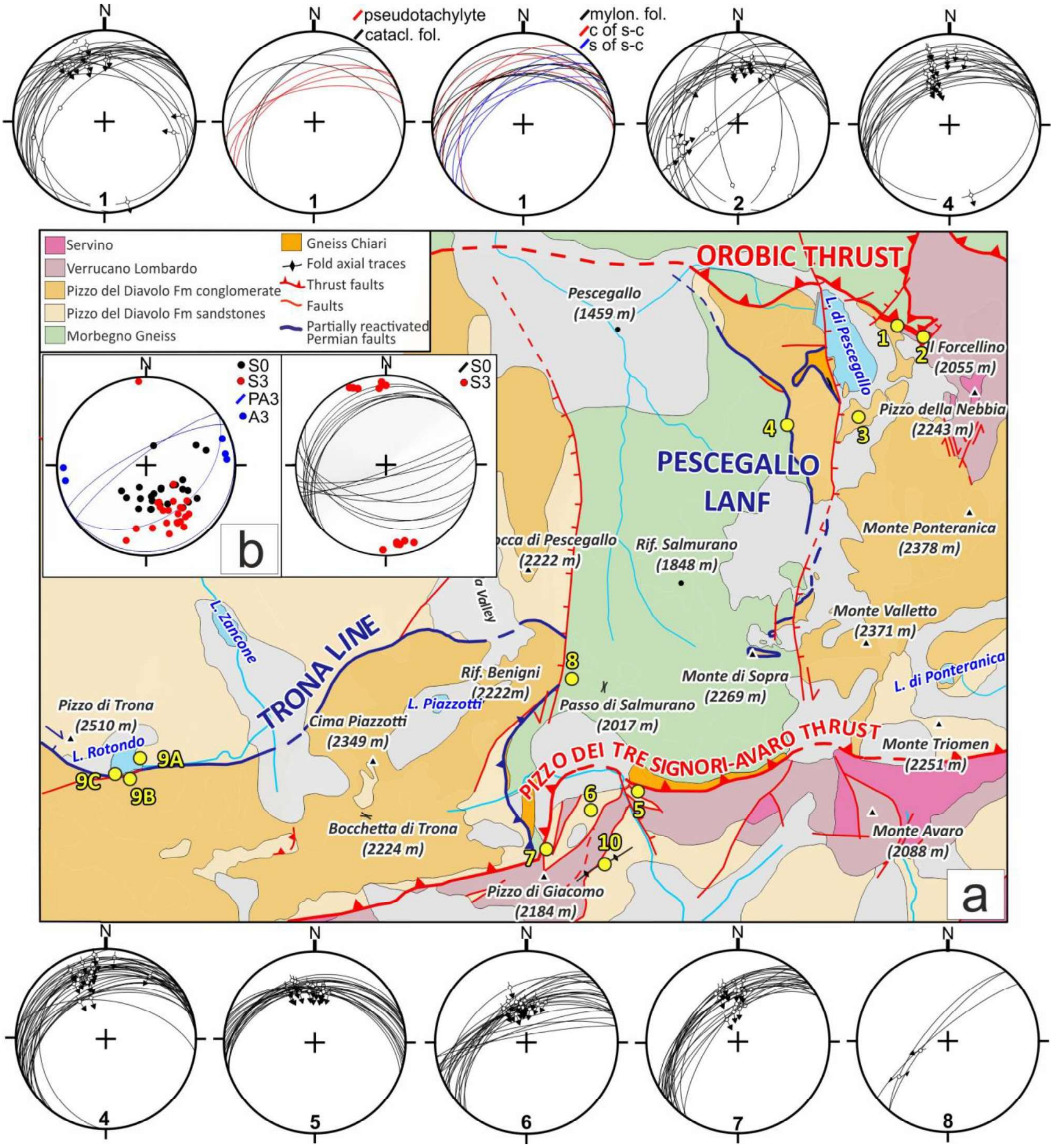

pseudotachylyte
catacl. fol.
mylon. fol.
c of s-c
s of s-c
Servino
Verrucano Lombardo
Pizzo del Diavolo Fm conglomerate
Pizzo del Diavolo Fm sandstones
Morbegno Gneiss
Gneiss Chiari
Fold axial traces
Thrust faults
Faults
Partially reactivated Permian faults
S0
S3
PA3
A3
OROBIC THRUST
PESCEGALLO LANF
TRONA LINE
PIZZO DEI TRE SIGNORI-AVARO THRUST
Pescegallo (1459 m)
L. di Pescegallo
Il Forcellino (2055 m)
Pizzo della Nebbia (2243 m)
Monte Ponteranica (2378 m)
Rif. Salmurano (1848 m)
Monte Valletto (2371 m)
Monte di Sopra (2269 m)
L. di Ponteranica
Monte Triomen (2251 m)
Monte Avaro (2088 m)
Passo di Salmurano (2017 m)
Rif. Benigni (2222m)
L. Piazzotti
Cima Piazzotti (2349 m)
Bocchetta di Trona (2224 m)
Pizzo di Giacomo (2184 m)
Pizzo di Trona (2510 m)
L. Rotondo
L. Zancone
Valley
(2222 m)
a
b


**Fig. 4**

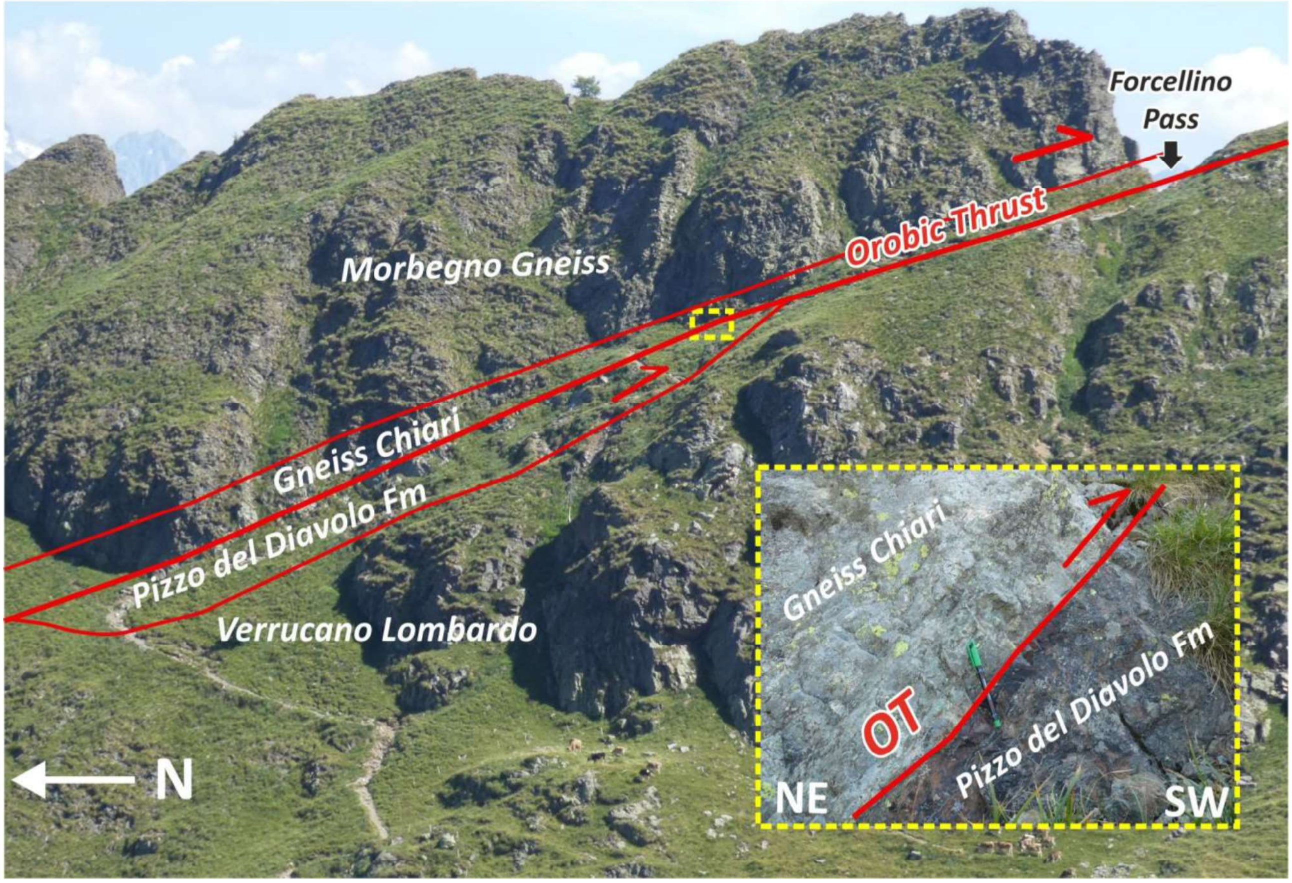
Forcellino
Pass
Orobic Thrust
Morbegno Gneiss
Gneiss Chiari
Pizzo del Diavolo Fm
Verrucano Lombardo
N
Gneiss Chiari
OT
Pizzo del Diavolo Fm
NE
SW
**Fig. 5**

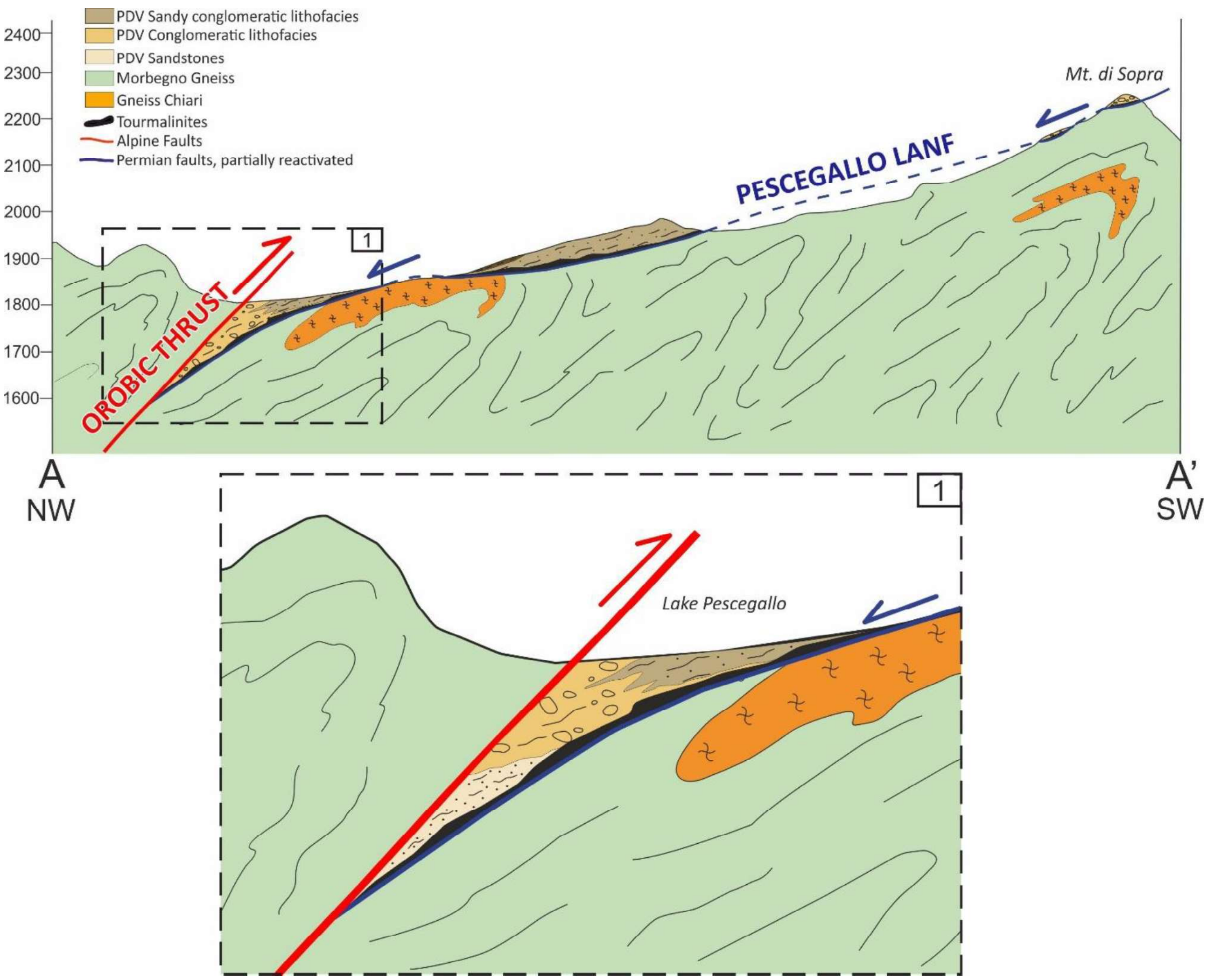
PDV Sandy conglomeratic lithofacies
PDV Conglomeratic lithofacies
PDV Sandstones
Morbegno Gneiss
Gneiss Chiari
Tourmalinites
Alpine Faults
Permian faults, partially reactivated
2400
2300
2200
2100
2000
1900
1800
1700
1600
Mt. di Sopra
PESCEGALLO LANF
OROBIC THRUST
1
A
NW
A'
SW
1
Lake Pescegallo

**Fig. 6**

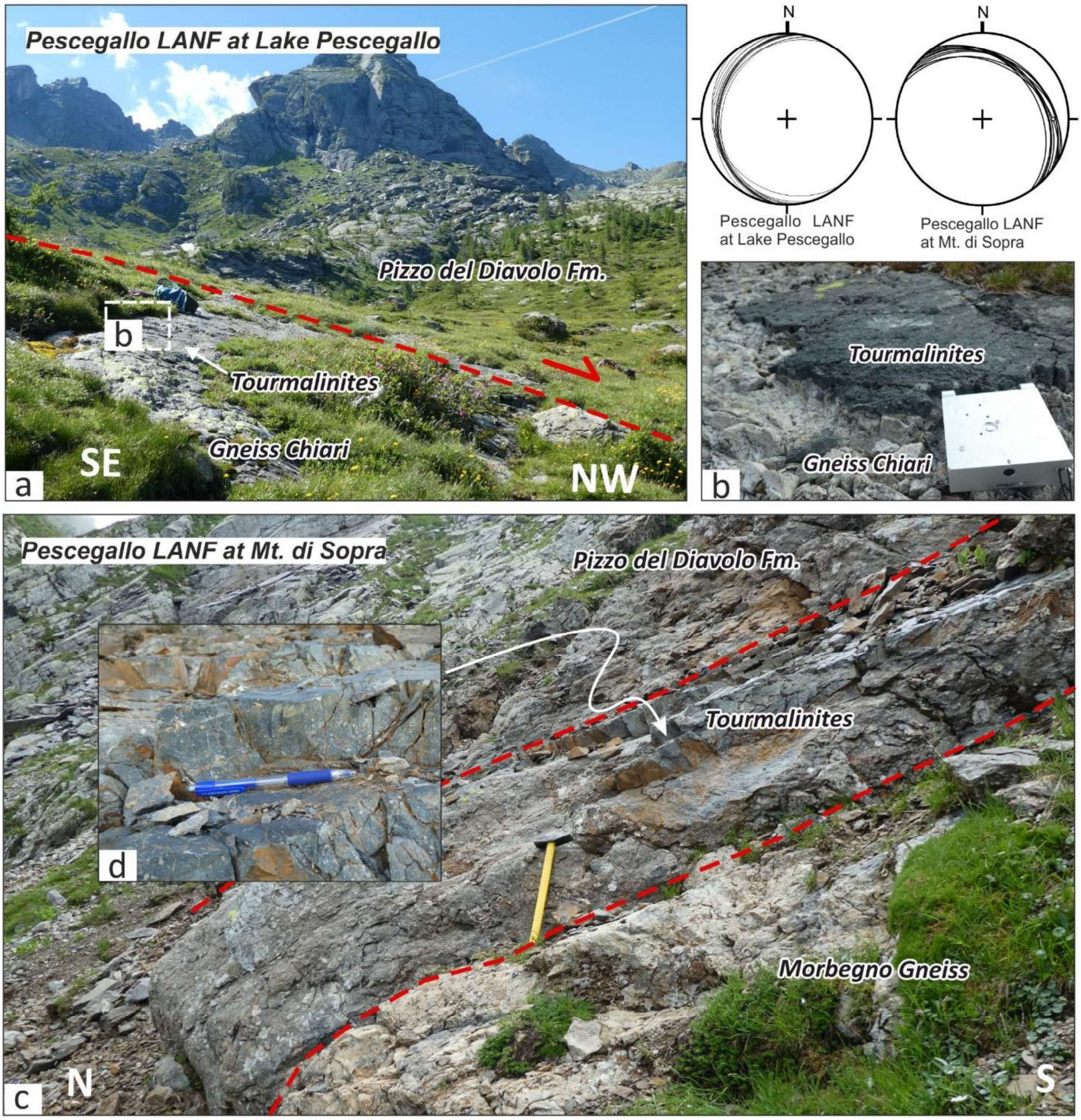

Pescegallo LANF at Lake Pescegallo
Pizzo del Diavolo Fm.
b
Tourmalinites
Gneiss Chiari
SE
NW
a
N
N
Pescegallo LANF
at Lake Pescegallo
Pescegallo LANF
at Mt. di Sopra
Tourmalinites
Gneiss Chiari
b
Pescegallo LANF at Mt. di Sopra
Pizzo del Diavolo Fm.
Tourmalinites
d
Morbegno Gneiss
c
N
S


**Fig. 7**

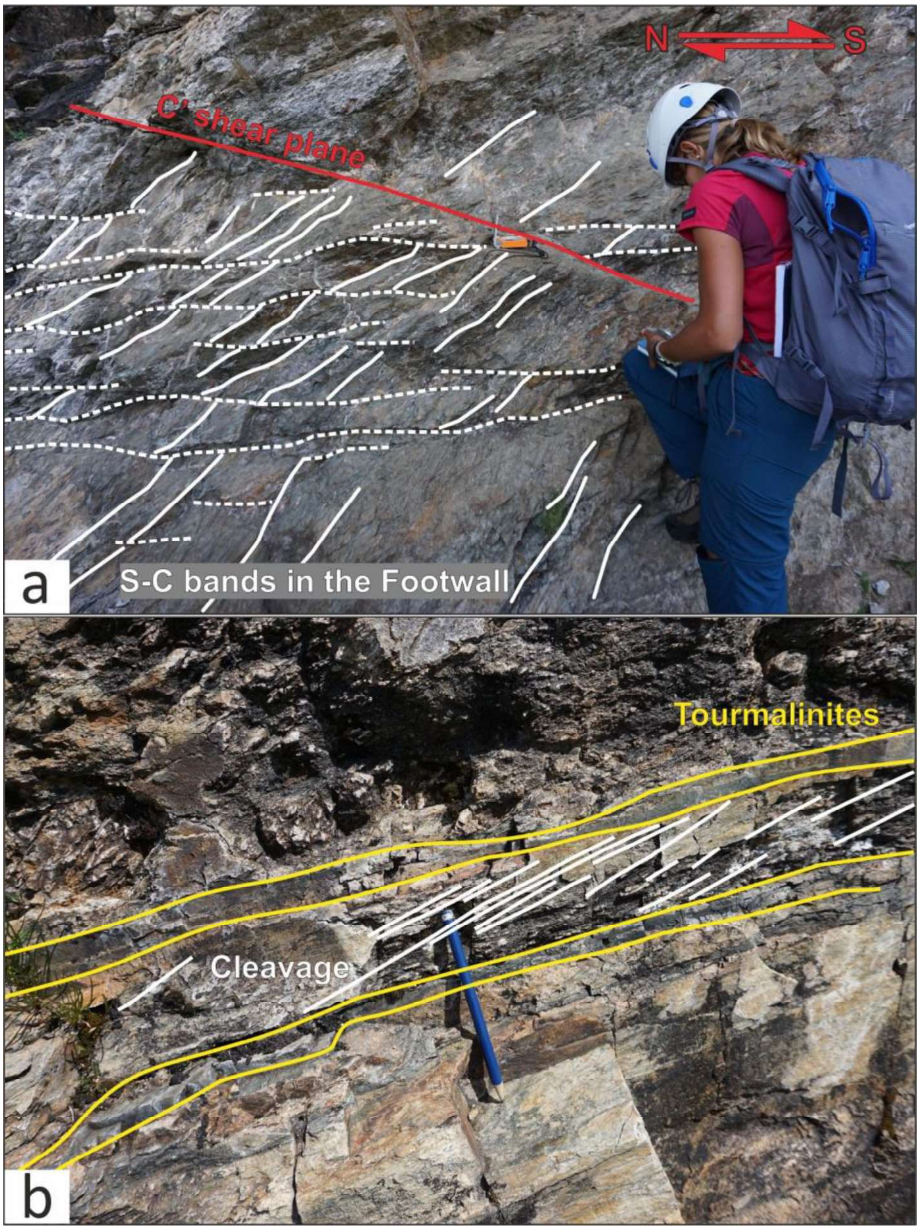
N
S
C' shear plane
a
S-C bands in the Footwall
Tourmalinites
Cleavage
b

Fig. 8

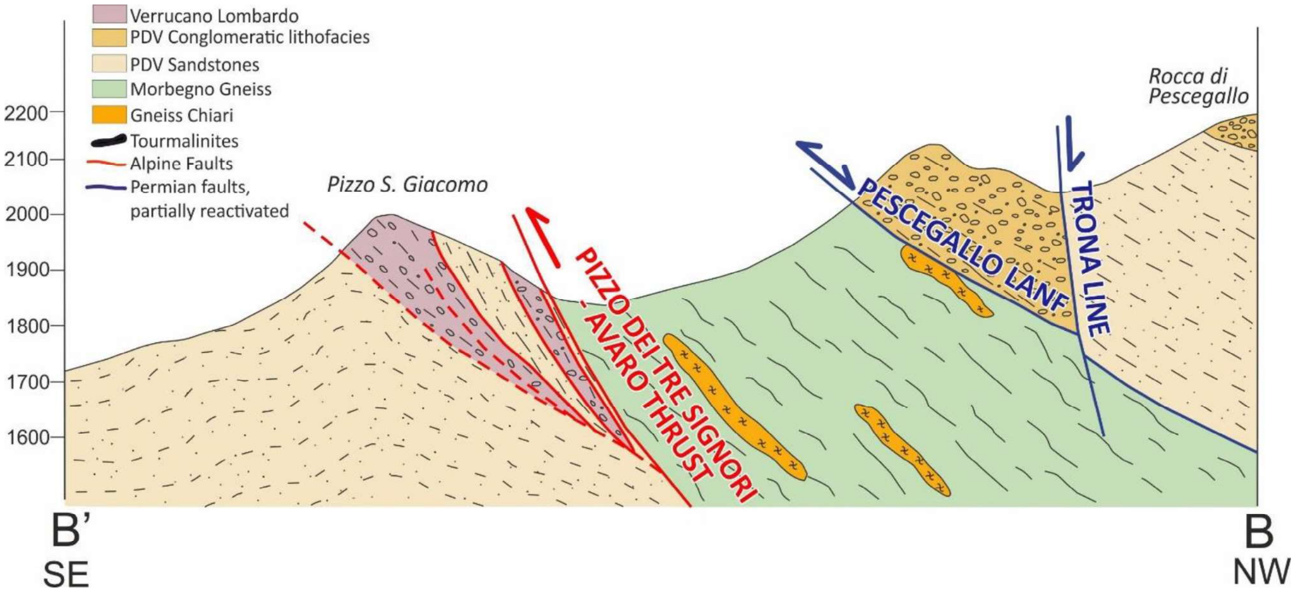
Verrucano Lombardo
PDV Conglomeratic lithofacies
PDV Sandstones
Morbegno Gneiss
Gneiss Chiari
Tourmalinites
Alpine Faults
Permian faults, partially reactivated
2200
2100
2000
1900
1800
1700
1600
Pizzo S. Giacomo
PIZZO DEI TRE SIGNORI - AVARO THRUST
PESCEGALLO LANF
TRONA LINE
Rocca di Pescegallo
B'
SE
B
NW
**Fig. 9**

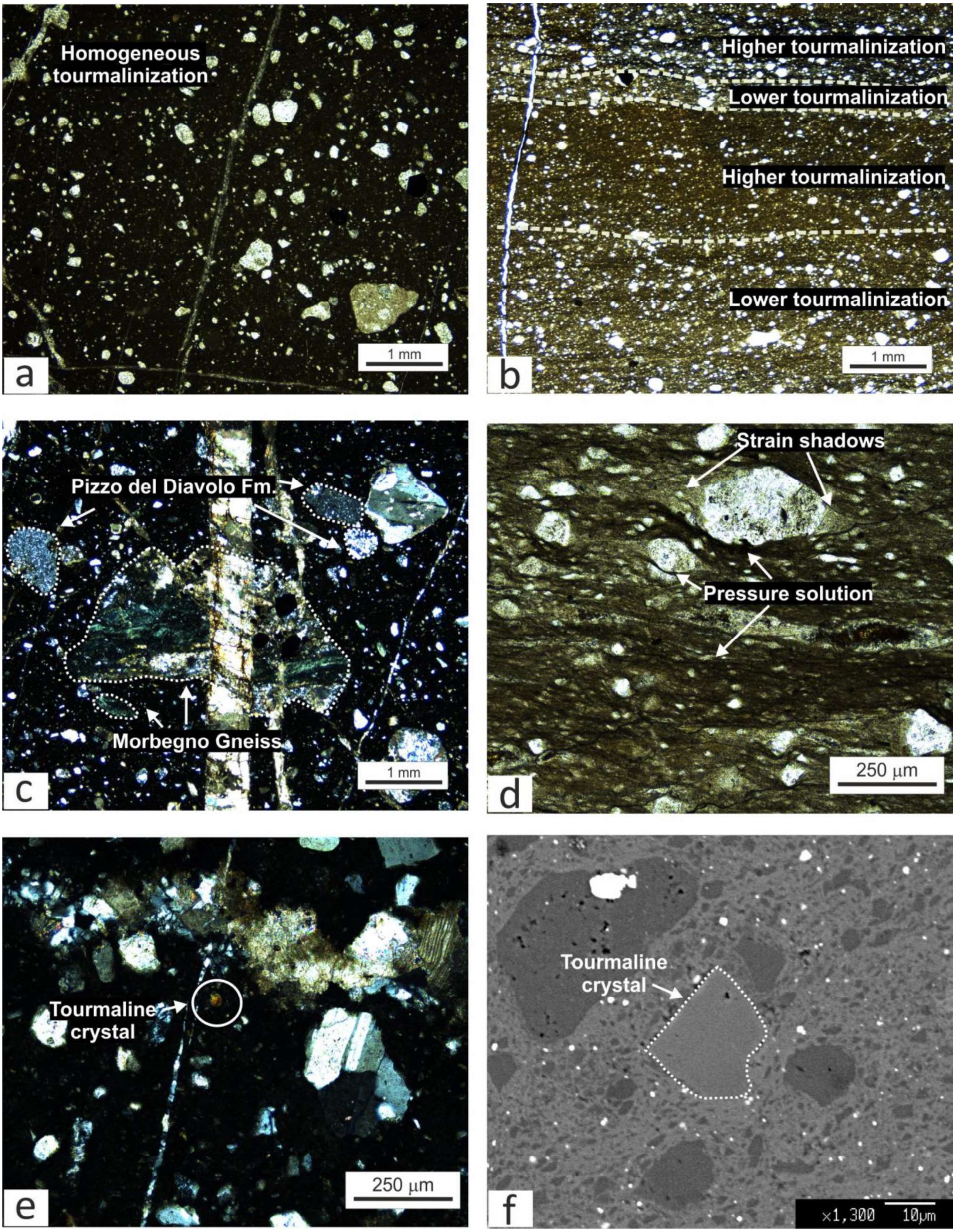

Homogeneous tourmalinization
1 mm
a
Higher tourmalinization
Lower tourmalinization
Higher tourmalinization
Lower tourmalinization
1 mm
b
Pizzo del Diavolo Fm.
Morbegno Gneiss
1 mm
c
Strain shadows
Pressure solution
250 μm
d
Tourmaline crystal
250 μm
e
Tourmaline crystal
×1,300 10μm
f


Fig. 10

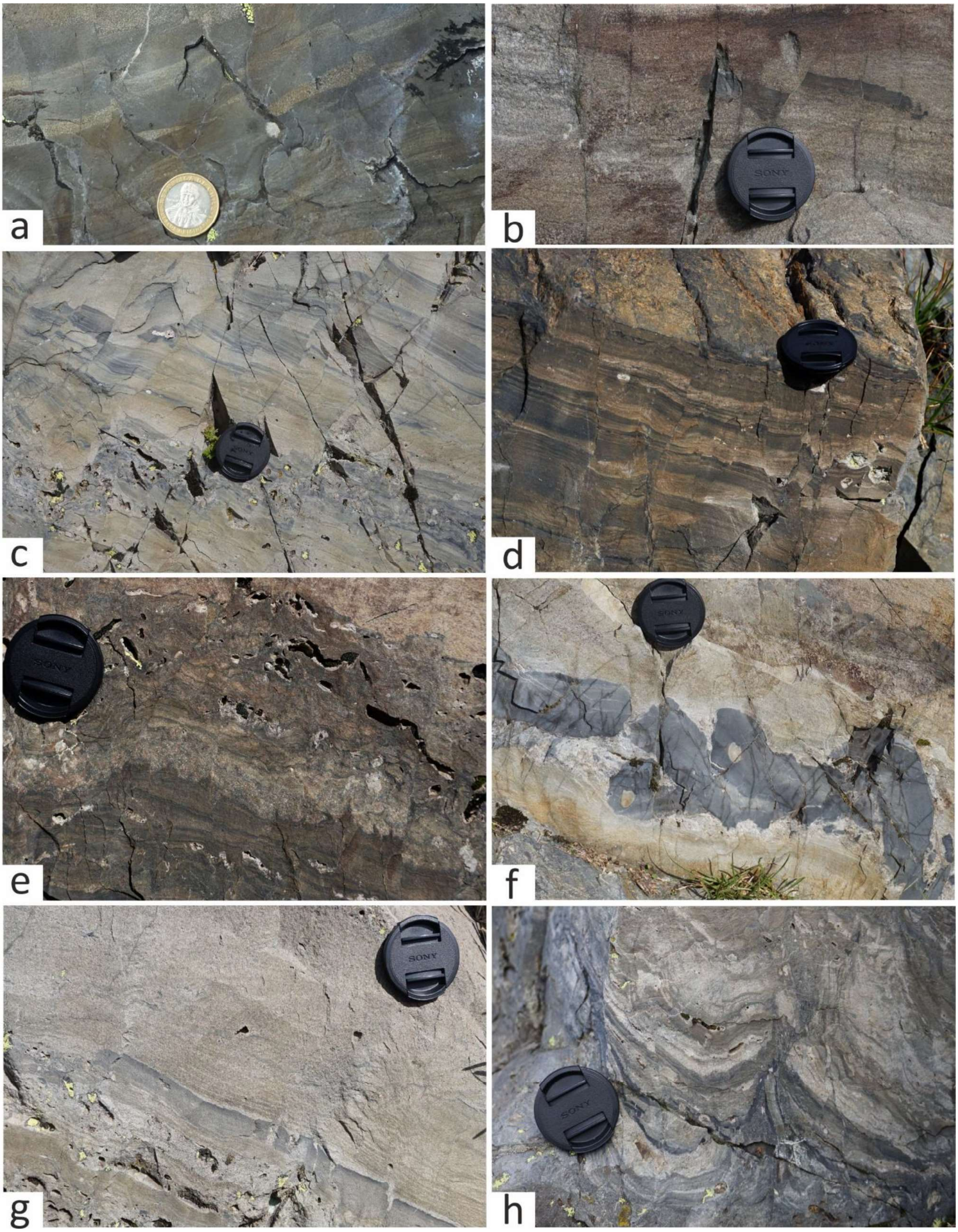

**Fig. 11**

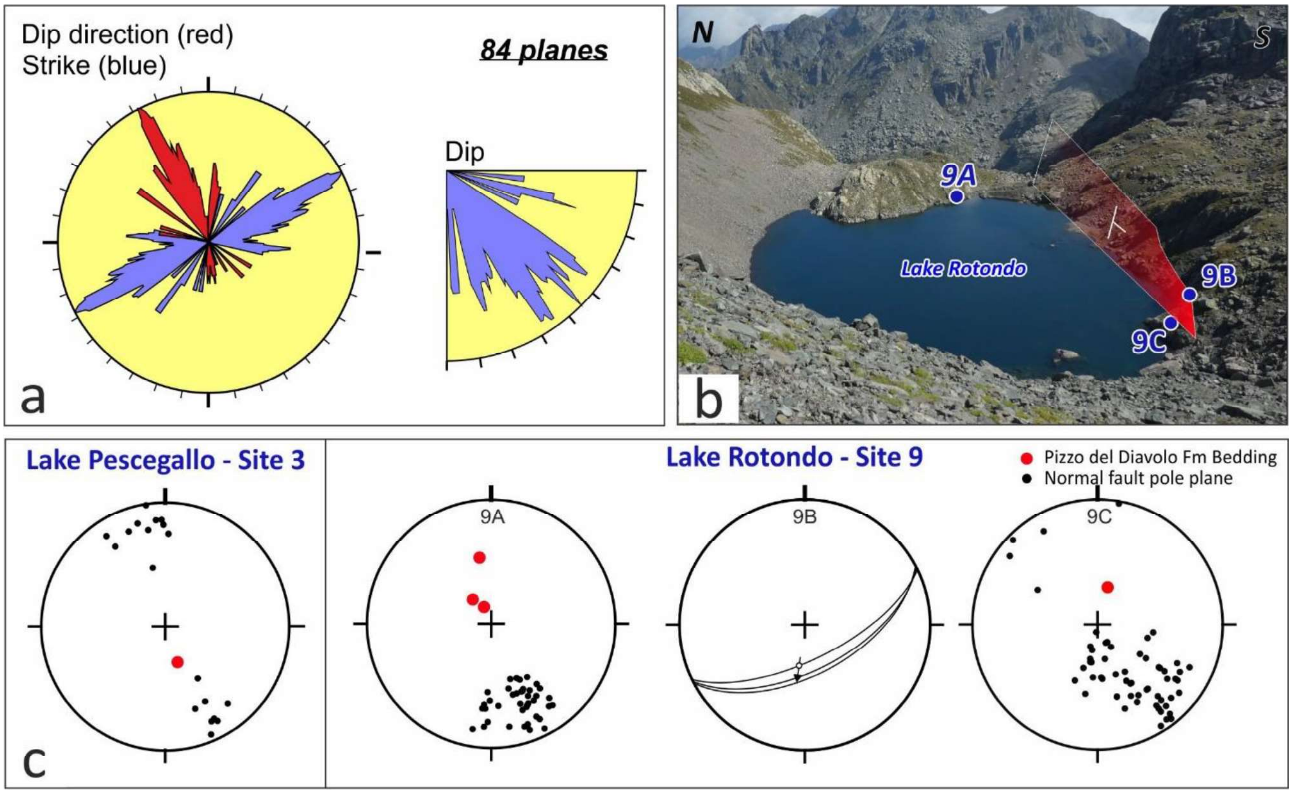
Dip direction (red)
Strike (blue)
84 planes
Dip
a
N
S
9A
Lake Rotondo
9B
9C
b
Lake Pescegallo - Site 3
Lake Rotondo - Site 9
Pizzo del Diavolo Fm Bedding
Normal fault pole plane
9A
9B
9C
c

Fig. 12

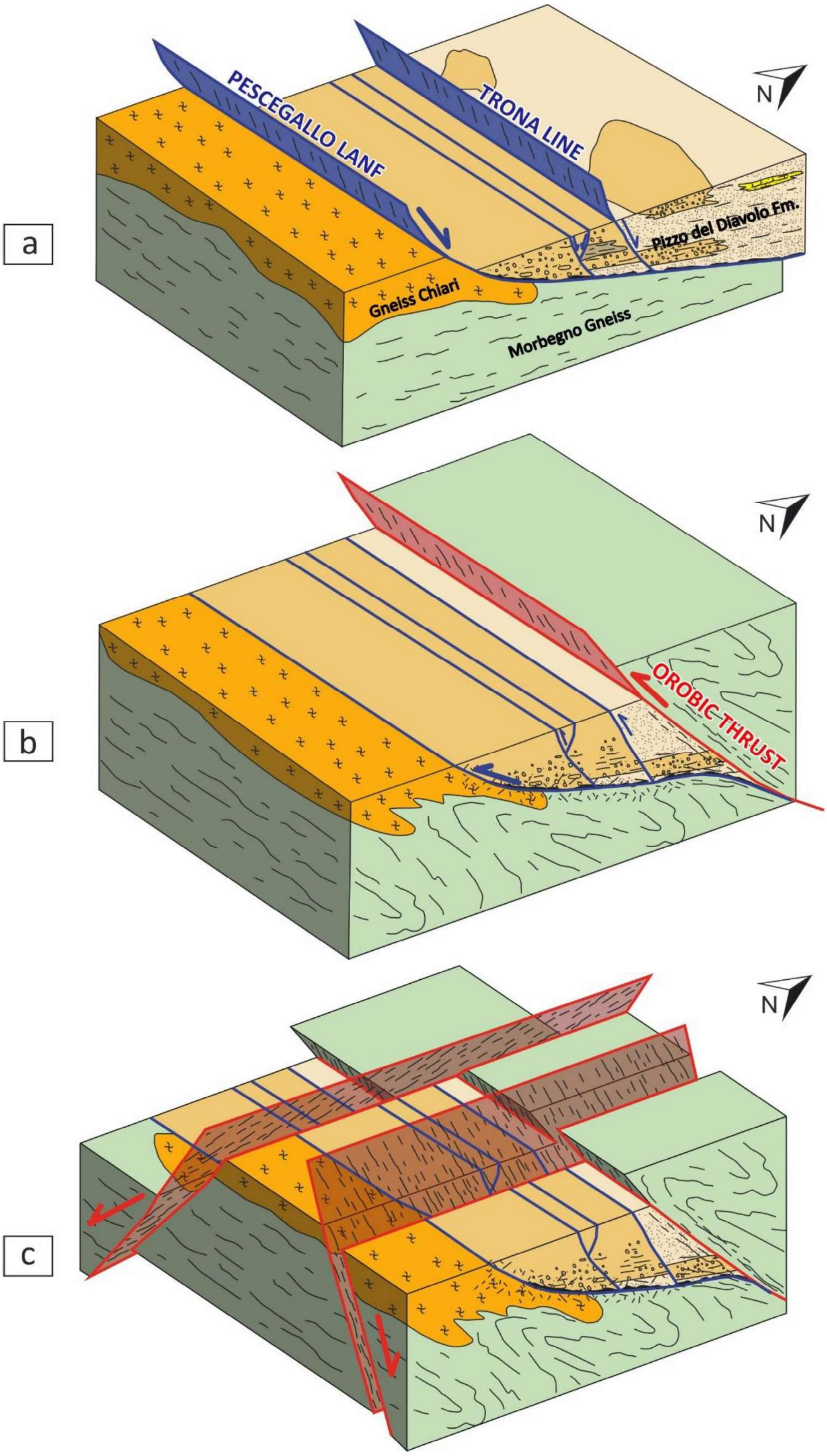

PESCEGALLO LANF
TRONA LINE
N
Pizzo del Diavolo Fm.
Gneiss Chiari
Morbegno Gneiss
a
OROBIC THRUST
b
c


**Fig. 13**